

Transport in polymer-gel composites: theoretical methodology and response to an electric field

By REGHAN J. HILL

Department of Chemical Engineering and McGill Institute for Advanced Materials, McGill University,
Montreal, Quebec, H3A 2B2, Canada

(Received 23 February 2005 and in revised form 22 August 2005)

A theoretical model of electromigrative, diffusive and convective transport in polymer-gel composites is presented. Bulk properties are derived from the standard electrokinetic model with an impenetrable charged sphere embedded in an electrolyte-saturated Brinkman medium. Because the microstructure can be carefully controlled, these materials are promising candidates for enhanced gel-electrophoresis, chemical sensing, drug delivery, and microfluidic pumping technologies. The methodology provides solutions for situations where perturbations from equilibrium are induced by gradients of electrostatic potential, concentration and pressure. While the volume fraction of the inclusions should be small, Maxwell's well-known theory of conduction suggests that the model may also be accurate at moderate volume fractions. In this work, the theory is used to compute ion fluxes, electrical current density, and convective flow driven by an electric field applied to an homogeneous composite. The electric-field-induced (electro-osmotic) flow is a sensitive indicator of the inclusion ζ -potential and size, electrolyte concentration, and Darcy permeability of the gel, while the electrical conductivity is usually independent of the polymer gel and is relatively insensitive to characteristics of the inclusions and electrolyte.

1. Introduction

Gel-electrophoresis is widely used to sort macromolecules based on their size and electrical charge. Selectivity to size is achieved by adjusting the permeability of the gel (e.g. agarose or polyacrylamide) through the concentrations of monomer, cross-linker, catalyst and initiator used in the gel synthesis. Molecular sorting based on other characteristics, such as receptor–ligand binding affinity, requires the gel to exhibit specific physicochemical activity. One way to achieve this in a controlled manner is to embed surface-functionalized particles (e.g. biological cells, and synthetic polymer or silica spheres) in a conventional polymer gel. Accordingly, this work seeks to quantify the influence of surface charge on transport driven by gradients of chemical and electrostatic potential. While the task is simplified to some extent by limiting the analysis to simple electrolytes whose mobilities are unhindered by the polymer gel, the methodology provides a significant step toward a theory that also accounts for hindered transport of larger electrolyte ions (e.g. proteins and DNA fragments).

This work also provides a quantitative interpretation of novel diagnostic tests – analogous to well-established microelectrophoresis and conductivity measurements – that probe the surface charge or ζ -potential of immobilized colloids in electrolytes where

the particles would otherwise aggregate. Attractive particle-interaction potentials arise when the solution pH approaches the isoelectric point of the particle–electrolyte interface, or the surface charge is sufficiently well screened by added salt (Russel, Saville & Schowalter 1989). By immobilizing colloids in an (ideally) inert (uncharged) polymer gel, at a pH and ionic strength where the interactions are repulsive, the pH and ionic strength may be varied without inducing coagulation.

Membranes of sintered glass beads (without intervening polymer) have long been used in ion-selective electrodes, and, more recently, as electro-osmotic pumps (e.g. Yao *et al.* 2003). Their simple design (no moving parts) and high-pressure low-flow characteristics are ideally suited to microfluidic applications. Filling the void space with a permeable, uncharged polymer gel, as proposed in this work, will increase viscous dissipation and, therefore, diminish pumping efficiency. Nevertheless, because applications are envisioned where poor pumping efficiency might be tolerated in view of other attributes, a quantitative analysis of electro-osmotic pumping is undertaken here.

The charge on particles dispersed in an electrolyte endows them with an electrophoretic mobility (Russel *et al.* 1989). Theoretical interpretation of the mobility (O'Brien & White 1978), sedimentation potential (Saville 1982), low-frequency conductivity (Saville 1979; O'Brien 1981), dielectric response (complex conductivity) (DeLacey & White 1981), and electroacoustic response (dynamic mobility) (O'Brien 1988, 1990) is widely used to infer the surface charge and, therefore, to indicate dispersion stability. Closely related are streaming-potential and streaming-current devices, which are used to infer the charge on macroscopic substrates, and the charge density and permeability of porous plugs and coatings (e.g. Hunter 2001; Dukhin, Zimmerman & Werner 2004).

This paper addresses a new but related problem in which impenetrable spheres with surface charge are randomly dispersed and immobilized in a permeable, electrolyte-saturated polymer gel (see figure 1). The transport processes that take place with the application of average (macroscale) gradients of electrostatic potential, electrolyte concentration and pressure are derived. While transport of electrolyte ions is relatively straightforward to calculate in an homogeneous, uncharged gel, charged inclusions disturb the applied fields, and applied fields disturb the equilibrium state of the diffuse double layers, so the resulting fluxes reflect a complex coupling of electromigration, diffusion, and convective transport.

Electrokinetic theories are often based on the *standard electrokinetic model* (Overbeek 1943; Booth 1950), whereby continuum equations governing the electric field, mobile charge (microions), mass, and momentum are solved with appropriate boundary conditions. The principal difficulty usually lies in capturing double-layer polarization and relaxation at surfaces whose radius of curvature is comparable to or smaller than the equilibrium double-layer thickness (Debye length). For 'bare' and 'soft' (polymer-coated) particles, polarization and relaxation can be addressed with novel numerical methodologies (O'Brien & White 1978; Hill, Saville & Russel 2003). In this work, a numerically exact solution of the problem is achieved for the low-volume-fraction limit where particle interactions can be neglected. The methodology also neglects quadratic and higher-order perturbations to the equilibrium state, providing *asymptotic coefficients* that characterize the far-field (power-law) decays of the velocity disturbance and perturbations to the equilibrium electric field and ion concentrations. In turn, the asymptotic coefficients are linked to bulk properties of the composite. The analysis resembles Maxwell's theory for the effective conductivity of a dilute, random configuration of spherical inclusions.

Dipolar disturbances† arise in the limit where the inclusions are uncharged. Then, with the application of a uniform electric field, the perturbed electrostatic potential ψ' reflects the non-conducting (impenetrable) surface of the inclusions, satisfying $\nabla^2\psi' = 0$. Similarly, when subjected to a bulk concentration gradient, the perturbed ion concentrations n' satisfy $\nabla^2 n' = 0$. In both cases, there is no convective flux, because the electrolyte is everywhere electrically neutral. With a uniform pressure gradient $\langle \nabla p \rangle$, the problem simplifies to the flow of an incompressible Newtonian fluid through a Brinkman medium with impenetrable inclusions. The (solenoidal) velocity \mathbf{u} satisfies $\eta \nabla^2 \mathbf{u} - \nabla p - (\eta/\ell^2)\mathbf{u} = \mathbf{0}$, where p is the pressure, η is the fluid viscosity, and ℓ is the Brinkman screening length (square root of the Darcy permeability). When the inclusion radius $a \gg \ell$, $\mathbf{u} = -(\ell^2/\eta)\nabla p$ with $\nabla^2 p = 0$ (Darcy flow), and the drag force on the inclusions is $2\pi\eta U a^3 \ell^{-2}$, where $\mathbf{U} = -(\ell^2/\eta)\langle \nabla p \rangle + O(\phi)$ is the average fluid velocity. In this limit, the inclusion contribution to the average drag force (per unit volume) of the composite is $n2\pi\eta U a^3 \ell^{-2} = (3/2)\phi\eta U \ell^{-2}$, where n is the inclusion number density and $\phi = n(4/3)\pi a^3$ is the volume fraction. With the same far-field velocity, the drag force on each inclusion is clearly much greater than the Stokes drag force $6\pi\eta a U$. Note also that the velocity disturbances $\mathbf{u}' = \mathbf{u} - \mathbf{U} = -(1/2)a^3 U_j (\delta_{ij} r^{-3} - 3x_i x_j r^{-5})$ decay as r^{-3} when the distance from the inclusions $r \gg a \gg \ell$.

When the inclusions are charged, a diffuse layer of mobile counter-ions envelops each inclusion, and electroneutrality demands that the net charge in the diffuse layers balances the immobile surface charge. With an applied electric field, the electrical body force within the diffuse layers drives an ‘inner’ flow which, in turn, drives an $O(\phi)$ ‘outer’ flow, with an $O(1)$ contribution due to an imposed pressure gradient. The electric-field-induced velocity disturbances ‘pump’ fluid through the polymer gel without exerting a net force on the composite. While the velocities are very low, composites with a 1 cm^2 cross-section can produce velocities of several microns per second in a microchannel. Note that a pressure gradient is necessary to overcome the drag required to pump fluid through an external network. However, the pressure-driven contribution to the flow is often small compared to the electric-field-induced flow. Under these conditions, the electric-field-induced flow rate is practically independent of the pressure gradient, and the maximum pressure gradient that can be sustained is limited by the strength of the composite and its support.

Ion fluxes manifest in an electrical current and, hence, a measurable electrical conductivity. Following earlier treatments of the low-frequency conductivity of dilute colloidal dispersions (Saville 1979; O’Brien 1981), the incremental contribution of the inclusions to the effective conductivity is calculated. These results link conductivity measurements to the particle surface charge density, for example. Because the fluxes are dominated by electromigration, the conductivity is not significantly influenced by the gel.

The model also provides the effective diffusivities of electrolyte ions when the bulk electrolyte concentration varies slowly in space and time. In a companion paper (Hill 2006), two important situations are examined: (i) bulk diffusion in the absence of an average electric field, and (ii) bulk diffusion with an electric field yielding zero current density. The former provides a simple setting in which to demonstrate the influence of the inclusions on the effective ion diffusion coefficients, whereas the latter provides the particle contribution to the membrane diffusion potential, which is well known in

† Here, *dipolar* refers to axisymmetric disturbances, without a source, that satisfy Laplace’s equation; these take the form $\alpha_j \partial r^{-1} / \partial x_j = -\alpha_i x_j r^{-3}$, where $r = |\mathbf{x}|$ and α_i are the components of a constant vector.

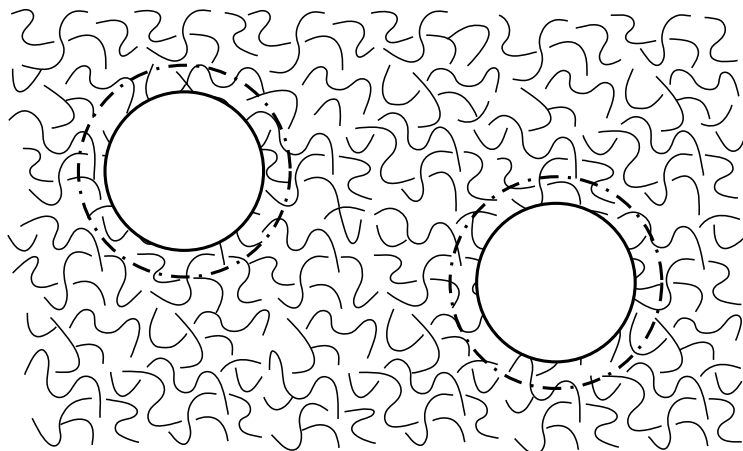


FIGURE 1. Schematic of the microscale system under consideration. Charged, impenetrable inclusions (solid circles) with radius $a \sim 10 \text{ nm} - 10 \mu\text{m}$ are embedded in a continuous polymer gel (solid filaments) saturated with aqueous electrolyte. Diffuse double layers (dash-dotted circles) with thickness $\kappa^{-1} \sim 1 - 100 \text{ nm}$ are perturbed by the application of an average electric field $-\langle \nabla \psi \rangle$, pressure gradient $\langle \nabla p \rangle$, or electrolyte concentration gradient $\langle \nabla n_j \rangle$. The Brinkman screening length $\ell \sim 1 - 10 \text{ nm}$ that specifies the Darcy permeability ℓ^2 of the gel is often small compared to the radius of the inclusions.

the fields of membrane biology, electrochemistry, and electrochemical engineering. In both cases, the particle contribution to these bulk properties may be comparable to or larger than in the absence of inclusions.

The paper is organized as follows. We begin in §2 with a description of the electrokinetic model. First, the composite microstructure and an apparatus for comparing theory and experiment are described. The subsections therein present the electrokinetic transport equations (§2.1), which are used to compute linearly independent solutions of the single-particle (microscale) problem (§2.2). Asymptotic coefficients from solutions of the microscale problem capture far-field decays of perturbations to the equilibrium state. These are used to calculate bulk ion fluxes in §2.3, and to derive an average momentum equation in §2.4. Results are presented in §3 for composites with negatively charged inclusions in polymer gels saturated with NaCl electrolyte. The subsections therein examine the incremental pore mobility (§3.1), electro-osmotic pumping (§3.2), incremental pressure gradient (§3.3) and, finally, species fluxes (§3.4) and electrical conductivity (§3.5). A brief summary follows in §4.

2. Theory

The microstructure of the composites considered in this work is depicted in figure 1. The continuous phase is a porous medium composed of an electrically neutral, electrolyte-saturated polymer gel. A *gel* refers to a network of polymer chains that is cross-linked so as to exhibit a solid-like (elastic) response to an applied stress. Polyacrylamide gels are routinely used for the electrophoretic separation of DNA segments in aqueous media. Their porosity may be controlled by adjusting the average densities and ratio of the monomer (acrylamide) and cross-linker. In this work, the hydrodynamic permeability is characterized by the Darcy permeability ℓ^2 (square of the Brinkman screening length), which reflects the hydrodynamic size a ,

and concentration n_s of the polymer segments. In turn, these reflect the degree of cross-linking and the affinity of the polymer for the solvent.

Embedded in the polymer are randomly dispersed spherical inclusions. In model systems, the inclusions are envisioned to be monodisperse silica or polymeric spheres, which typically have radii in the range $a = 10 \text{ nm} - 10 \mu\text{m}$ and bear a surface charge when dispersed in aqueous media. The surface charge density may vary with the bulk ionic strength and pH of the electrolyte. In this work, however, the surface charge is to be inferred from the bulk ionic strength and surface potential ζ . Because the inclusions are impenetrable with zero surface capacitance and conductivity, no-flux and no-slip boundary conditions apply at their surfaces.

Note that the mobile ions whose charge is opposite to the surface-bound immobile charge are referred to as *counter-ions*, with the other species referred to as *co-ions*. For simplicity, the counter-charges, i.e. the dissociated counter-ions, are assumed indistinguishable from the electrolyte counter-ions. Surrounding each inclusion is a diffuse layer of mobile charge, with Debye thickness κ^{-1} and excess of counter-ions. As described below, the layer structure is calculated from the well-known Poisson–Boltzmann equation.

In this work, the polymer gel is assumed not to hinder ion motion. For larger ions and dense polymer gels, the influence of the network on the diffusive, electromigrative and convective fluxes may be modelled with an equation of motion for an ion

$$\gamma(\mathbf{u} - \mathbf{v}) - \gamma'\mathbf{v} + \mathbf{f} = \mathbf{0}, \quad (2.1)$$

where the first term represents the hydrodynamic drag due to relative motion, \mathbf{u} and \mathbf{v} are the (average) fluid and ion velocities, and γ is the friction coefficient. The second term approximates the force exerted by the polymer gel on the ion, with the friction coefficient γ' reflecting the relative size of the ion and polymer interstices. The third term accounts for electrical and thermal (Brownian) forces, depending on the time-scale of interest. The unhindered ion velocity is $\mathbf{v}^0 = \mathbf{u} + \mathbf{f}/\gamma$, so the hindered velocity may be written $\mathbf{v} = \mathbf{v}^0\gamma/(\gamma + \gamma')$. Therefore, under steady conditions, the ion conservation equation $\nabla \cdot (n\mathbf{v}) = 0$ is independent of γ' (n is the ion number density). When $\mathbf{u} = \mathbf{0}$, for example, the ion will diffuse (or electromigrate) with an *effective* diffusivity (or mobility) $D^e = D\gamma/(\gamma + \gamma')$, where D is the unhindered diffusivity. It follows that $\mathbf{v} = \mathbf{v}^0 D^e/D$, so the hindered flux equals the unhindered flux multiplied by the ratio of the hindered to unhindered ion diffusivities (mobilities).

Now consider the influence of hindered ion migration on the fluid momentum conservation equation. From (2.1), the (hydrodynamic drag) force exerted by an ion on the solvent is

$$\gamma(\mathbf{v} - \mathbf{u}) = (\mathbf{f} - \gamma'\mathbf{u})\gamma/(\gamma + \gamma'), \quad (2.2)$$

where $\mathbf{f} = -ze\nabla\psi$ is the electrical force on the ion (z is the valance, e is the elementary charge, and ψ is the electrostatic potential). It follows that the net force (per unit volume) exerted by the ions on the fluid is

$$-\sum_{j=1}^N n_j(\gamma'_j\mathbf{u} + z_j e\nabla\psi)D_j^e/D_j, \quad (2.3)$$

where the sum is over all N ion species. Clearly, as $\gamma'_j/\gamma_j \rightarrow 0$ when the hindrance of the polymer is negligible, ions transfer their electrical force to the fluid. As $\gamma'_j/\gamma_j \rightarrow \infty$, however, immobilized ions transfer the electrical force to the polymer, so the net force exerted by each ion on the fluid becomes $-\gamma_j\mathbf{u}$.

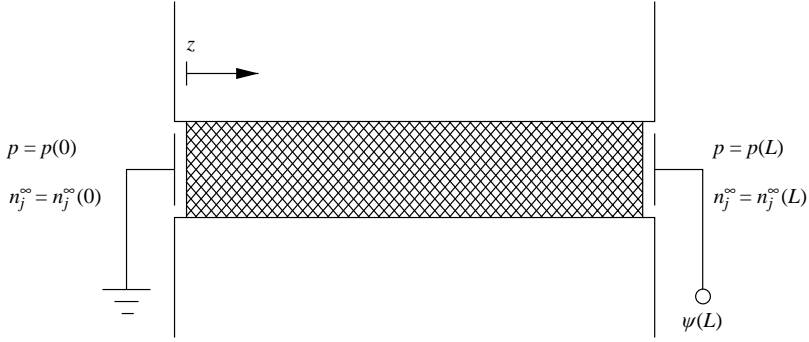


FIGURE 2. Schematic of the macroscale system under consideration. A polymer gel embedded with spherical charged inclusions (see figure 1) separates (by length L) two reservoirs containing electrolyte with different species concentrations ($n_j^\infty(z=0)$ and $n_j^\infty(z=L)$) and, possibly, pressures ($p(z=0)$ and $p(z=L)$). Electrodes on each side of the ‘bridge’ permit an electric field to be applied and the differential electrostatic potential $\Delta\psi = \psi(z=L) - \psi(z=0)$ to be measured. The walls of the bridge are impenetrable and non-conducting.

A simple apparatus to realize the conditions under which the theory may be applied is depicted in figure 2. The composite bridges two reservoirs, each, in general, with a different electrolyte concentration and pressure. Electrodes are placed at each end of the bridge, so either a uniform electric field can be established or an average electric field strength measured. The channel is to realize constant ion fluxes under steady or quasi-steady conditions. This makes the averaged microscale transport equations easier to solve, but, in general, the averaged equations apply to macroscale fluxes in two- and three-dimensional geometries when the (average) inclusion number density, ion concentrations, electric field and fluid velocity vary slowly in space and time.

2.1. The electrokinetic transport equations

The transport equations and boundary conditions are presented here in dimensional form. They comprise the nonlinear Poisson–Boltzmann equation

$$\epsilon_o \epsilon_s \nabla^2 \psi = - \sum_{j=1}^N (n_j - n_j^f) z_j e, \quad (2.4)$$

where ϵ_o and ϵ_s are the permittivity of a vacuum and dielectric constant of the electrolyte, n_j are the concentrations of the j th mobile ions with valences z_j , and ψ and e are the electrostatic potential and elementary charge. In this work, the polymer is uncharged, so the fixed charge density n_j^f is zero. For convenience, the valence of the fixed charge is set opposite to that of its respective (mobile) counter-ion in (2.4); this defines the concentration n_j^f .

Transport of the mobile ions is governed by

$$6\pi\eta a_j (\mathbf{u} - \mathbf{v}_j) - z_j e \nabla \psi - kT \nabla \ln n_j = 0 \quad (j = 1, \dots, N), \quad (2.5)$$

where a_j are Stokes radii of the ions, obtained from limiting conductances or diffusivities, η is the electrolyte viscosity, \mathbf{u} and \mathbf{v}_j are the fluid and ion velocities, and kT is the thermal energy.

Ion diffusion coefficients, which are adopted throughout this paper, are

$$D_j = kT / (6\pi\eta a_j). \quad (2.6)$$

As usual, the double-layer thickness (Debye length)

$$\kappa^{-1} = \sqrt{kT\epsilon_s\epsilon_o/(2Ie^2)} \quad (2.7)$$

emerges from (2.4) and (2.5) where,

$$I = (1/2) \sum_{j=1}^N z_j^2 n_j^\infty \quad (2.8)$$

is the bulk (average) ionic strength, with n_j^∞ the bulk ion concentrations.

Ion conservation demands

$$\partial n_j / \partial t = -\nabla \cdot (n_j \mathbf{v}_j) \quad (j = 1, \dots, N), \quad (2.9)$$

where t is the time, and the ion fluxes

$$\mathbf{j}_j = n_j \mathbf{v}_j = -D_j \nabla n_j - z_j e \frac{D_j}{kT} n_j \nabla \psi + n_j \mathbf{u} \quad (2.10)$$

are obtained from (2.5).

Similarly, momentum and mass conservation require

$$\rho_s \partial \mathbf{u} / \partial t = \eta \nabla^2 \mathbf{u} - \nabla p - (\eta / \ell^2) \mathbf{u} - \sum_{j=1}^N n_j z_j e \nabla \psi \quad (2.11)$$

and

$$\nabla \cdot \mathbf{u} = 0, \quad (2.12)$$

where ρ_s and \mathbf{u} are the electrolyte density and velocity, and p is the pressure. Note that $-(\eta / \ell^2) \mathbf{u}$ represents the hydrodynamic drag force exerted by the polymer on the electrolyte. The Darcy permeability ℓ^2 (square of the Brinkman screening length) of the gel may be expressed as

$$\ell^2 = 1 / [n_s(r) 6\pi a_s F_s] = 2a_s^2 / [9\phi_s(r) F_s(\phi_s)], \quad (2.13)$$

where $n_s(r)$ is the concentration of Stokes resistance centres, with a_s and $F_s(\phi_s)$ the Stokes radius and drag coefficient of the polymer segments. In this work, n_s is constant, but, in general, may vary with radial position r from the centre of each inclusion. Note also that the Brinkman screening length is adjusted according to (2.13) by varying the (uniform) polymer segment density with Stokes radius $a_s = 1 \text{ \AA}$. The drag coefficient F_s is obtained from a correlation developed by Koch & Sangani (1999) for random fixed beds of spheres. While the microstructure of a polymer gel is clearly not the same as that of a random bed of spheres, the model is intended to capture the significant influence of hydrodynamic interactions on the permeability when the volume fraction of polymer is not small. In this work, however, only the reported values of ℓ are relevant. For example, the value $\ell \approx 0.951 \text{ nm}$, which is adopted for the principal set of results tabulated below, reflects a polymer segment concentration n_s that yields $\ell = 1 \text{ nm}$ according to (2.13) when the Stokes radius $a_s = 1 \text{ \AA}$ and the drag coefficient $F_s = 1$. Because the hydrodynamic volume fraction $\phi_s = n_s(4/3)\pi a_s^3 > 0$, $F_s(\phi_s) > 1$ and, hence, ℓ is slightly less than the targeted value.

2.1.1. Inner (particle surface) boundary conditions

Either the equilibrium surface potential ζ or surface charge density σ may be specified. Because the surface ($r = a$) is assumed impenetrable with zero capacitance and conductivity, the surface charge is constant, permitting no-flux boundary

conditions for each (mobile) ion species. As usual, the no-slip boundary condition applies. It follows that (inner) boundary conditions are either

$$\psi = \zeta \text{ at } r = a \quad (2.14)$$

or

$$\epsilon_s \epsilon_o \nabla \psi|_{out} \cdot \hat{\mathbf{n}} - \epsilon_p \epsilon_o \nabla \psi|_{in} \cdot \hat{\mathbf{n}} = -\sigma \text{ at } r = a, \quad (2.15)$$

with

$$n_j \mathbf{v}_j \cdot \hat{\mathbf{n}} = 0 \text{ at } r = a \quad (2.16)$$

and

$$\mathbf{u} = \mathbf{0} \text{ at } r = a, \quad (2.17)$$

where $\hat{\mathbf{n}} = \mathbf{e}_r$ is an outward unit normal and ϵ_p is the particle dielectric constant.

2.1.2. Outer (far-field) boundary conditions

Neglecting particle interactions requires far-field boundary conditions

$$\psi \rightarrow -\mathbf{E} \cdot \mathbf{r} \text{ as } r \rightarrow \infty, \quad (2.18)$$

$$n_j \rightarrow n_j^\infty + \mathbf{B}_j \cdot \mathbf{r} \text{ as } r \rightarrow \infty, \quad (2.19)$$

$$\mathbf{u} \rightarrow \mathbf{U} \text{ as } r \rightarrow \infty, \quad (2.20)$$

where \mathbf{E} , \mathbf{B}_j and \mathbf{U} are, respectively, a constant electric field, constant species concentration gradients, and constant far-field velocity.

2.2. Solution of the equations

2.2.1. Equilibrium state

When $\mathbf{E} = \mathbf{B}_j = \mathbf{U} = \mathbf{0}$, equilibrium is specified according to

$$\epsilon_o \epsilon_s \nabla^2 \psi^0 = - \sum_{j=1}^N (n_j^0 - n_j^f) z_j e, \quad (2.21)$$

$$0 = \nabla \cdot \left[D_j \nabla n_j^0 + z_j e \frac{D_j}{kT} n_j^0 \nabla \psi^0 \right], \quad (2.22)$$

$$0 = -\nabla p^0 - \sum_{j=1}^N n_j^0 z_j e \nabla \psi^0, \quad (2.23)$$

with boundary conditions

$$\psi^0 = \zeta \text{ at } r = a, \quad (2.24)$$

$$\epsilon_s \epsilon_o \nabla \psi^0|_{out} \cdot \mathbf{e}_r - \epsilon_p \epsilon_o \nabla \psi^0|_{in} \cdot \mathbf{e}_r = -\sigma \text{ at } r = a, \quad (2.25)$$

$$n_j^0 \left[D_j \nabla n_j^0 + z_j e \frac{D_j}{kT} n_j^0 \nabla \psi^0 \right] \cdot \mathbf{e}_r = 0 \text{ at } r = a, \quad (2.26)$$

and

$$\psi^0 \rightarrow 0 \text{ as } r \rightarrow \infty, \quad (2.27)$$

$$n_j^0 \rightarrow n_j^\infty \text{ as } r \rightarrow \infty. \quad (2.28)$$

2.2.2. Linearized perturbed state

Perturbations to the equilibrium state (above) are introduced via

$$\psi = \psi^0 - \mathbf{E} \cdot \mathbf{r} + \psi', \quad (2.29)$$

$$n_j = n_j^0 + \mathbf{B}_j \cdot \mathbf{r} + n'_j, \quad (2.30)$$

$$p = p^0 + \mathbf{P} \cdot \mathbf{r} + p', \quad (2.31)$$

where the first terms on the right-hand sides denote the equilibrium values, with the primed quantities denoting perturbations. Note that \mathbf{P} is the far-field pressure gradient required to sustain a far-field velocity $\mathbf{U} = -(\ell^2/\eta)\mathbf{P}$.

With ‘forcing’

$$\mathbf{X} = X\mathbf{e}_z, \quad (2.32)$$

where $X \in \{E, B_j, U\}$ (in general, a linear combination of these variables), the linearized perturbations are symmetric about the z -axis ($\theta = 0$) of a spherical polar coordinate system, taking the forms

$$\psi' = \hat{\psi}(r)\mathbf{X} \cdot \mathbf{e}_r, \quad (2.33)$$

$$n'_j = \hat{n}_j(r)\mathbf{X} \cdot \mathbf{e}_r, \quad (2.34)$$

$$\mathbf{u} = \mathbf{U} + \mathbf{u}', \quad (2.35)$$

where

$$\begin{aligned} \mathbf{u}' &= \nabla \times \nabla \times h(r)\mathbf{X} \\ &= -2(h_r/r)(\mathbf{X} \cdot \mathbf{e}_r)\mathbf{e}_r - (h_{rr} + h_r/r)(\mathbf{X} \cdot \mathbf{e}_\theta)\mathbf{e}_\theta. \end{aligned} \quad (2.36)$$

Equation (2.36) guarantees a solenoidal (incompressible) velocity field, which permits the momentum equation to be solved by applying the curl $\nabla \times$, thereby eliminating the pressure and yielding a scalar equation for the single non-zero component of the vorticity $\nabla \times \mathbf{u} = \omega_\phi \mathbf{e}_\phi$. The perturbations satisfy

$$\epsilon_o \epsilon_s \nabla^2 \psi' = - \sum_{j=1}^N (n'_j + \mathbf{B}_j \cdot \mathbf{r}) z_j e, \quad (2.37)$$

and

$$\nabla \cdot \mathbf{j}_j = 0, \quad (2.38)$$

where

$$\begin{aligned} \mathbf{j}_j &= -D_j(\nabla n'_j + \mathbf{B}_j) - z_j e \frac{D_j}{kT} (n'_j + \mathbf{B}_j \cdot \mathbf{r}) \nabla \psi^0 \\ &\quad - z_j e \frac{D_j}{kT} n_j^0 (\nabla \psi' - \mathbf{E}) + n_j^0 (\mathbf{U} + \mathbf{u}'), \end{aligned} \quad (2.39)$$

$$\begin{aligned} \eta \nabla^2 \mathbf{u}' - \nabla p' - (\eta/\ell^2)(\mathbf{U} + \mathbf{u}') - \sum_{j=1}^N n_j^0 z_j e (\nabla \psi' - \mathbf{E}) \\ - \sum_{j=1}^N (n'_j + \mathbf{B}_j \cdot \mathbf{r}) z_j e \nabla \psi^0 = 0, \end{aligned} \quad (2.40)$$

$$\nabla \cdot \mathbf{u}' = 0, \quad (2.41)$$

with boundary conditions

$$\epsilon_s \epsilon_o (\nabla \psi' - \mathbf{E})|_{out} \cdot \mathbf{e}_r - \epsilon_p \epsilon_o (\nabla \psi' - \mathbf{E})|_{in} \cdot \mathbf{e}_r = 0 \text{ at } r = a, \quad (2.42)$$

$$\left[D_j(\nabla n'_j + \mathbf{B}_j) + z_j e \frac{D_j}{kT} (n'_j + \mathbf{B}_j \cdot \mathbf{r}) \nabla \psi^0 + z_j e \frac{D_j}{kT} n_j^0 (\nabla \psi' - \mathbf{E}) - n_j^0 (\mathbf{U} + \mathbf{u}') \right] \cdot \mathbf{e}_r = 0 \text{ at } r = a, \quad (2.43)$$

$$\mathbf{u}' = -\mathbf{U} \text{ at } r = a, \quad (2.44)$$

and

$$\psi' \rightarrow (\mathbf{X} \cdot \mathbf{e}_r) D^X / r^2 \text{ as } r \rightarrow \infty, \quad (2.45)$$

$$n'_j \rightarrow (\mathbf{X} \cdot \mathbf{e}_r) C_j^X / r^2 \text{ as } r \rightarrow \infty, \quad (2.46)$$

$$\mathbf{u}' \rightarrow -2(C^X / r^3)(\mathbf{X} \cdot \mathbf{e}_r) \mathbf{e}_r - (C^X / r^3)(\mathbf{X} \cdot \mathbf{e}_\theta) \mathbf{e}_\theta \text{ as } r \rightarrow \infty. \quad (2.47)$$

In the far field, the velocity disturbance \mathbf{u}' is proportional to the gradient of ψ' , which, like the electrostatic potential and ion concentrations, is dipolar. Accordingly, \mathbf{u}' decays as r^{-3} , and D^X and C_j^X will often be referred to as the strength of the electrostatic and concentration polarization (or dipole moments) induced by the field $\mathbf{X} \in \{E, B_j, U\}$.

The dimensions of the asymptotic coefficients D^X , C_j^X and C^X , which depend on the respective $\mathbf{X} \in \{E, B_j, U\}$, are easily worked out by inspecting (2.45)–(2.47). For convenience, dimensionless values are presented in the tables in §3 below with a , $u^* = \epsilon_s \epsilon_o (kT/e)^2 / (\eta a)$, $2I$ and kT/e as the scales for length, velocity, ion concentrations and electrostatic potential, respectively.

2.2.3. Superposition

The equations are solved using a numerical methodology developed by Hill *et al.* (2003) for the electrophoretic mobility of polymer-coated colloids. Solutions with E , B_j and U set to arbitrary values can be computed, provided $\sum_{j=1}^N z_j B_j = 0$ to ensure an electrically neutral far field. However, when N species are assembled into M electroneutral groups (e.g. electrolytes or neutral tracers), each with far-field gradient B_k ($k = 1, \dots, M$), it is expedient to compute solutions with only one non-zero value of E , B_k or U . Then, arbitrary solutions can be obtained by linear superposition (O'Brien & White 1978).

An index k' is required to identify the (electroneutral) group to which the j th species under consideration is assigned. Careful consideration of the electrolyte composition and ion valences is required to ensure consistency. For z - z electrolytes it is convenient to set $B_j = B_k$, whereas for a single 2-1 electrolyte (e.g. CaCl_2) it is satisfactory to set $B_j = B_k / |z_j|$. For the relatively simple situations considered in this work, the (single) electroneutral group is NaCl , so $M = 1$ with $k = k' = 1$, and $j = 1$ and 2 for Na^+ and Cl^- , respectively.

Note that $C_j^{B_k}$, for example, is the asymptotic coefficient for the perturbed concentration of the j th species induced by the k th concentration gradient B_k , whereas C^{B_k} (without a subscript) denotes the asymptotic coefficient for the flow induced by B_k .

For neutral species, the concentration disturbance produced by a single impenetrable sphere yields $C_j^{B_{k'}} = (1/2)a^3$, otherwise $C_j^{B_k} = 0$ ($k \neq k'$). Clearly, the asymptotic coefficients for charged species, whose concentration perturbations are influenced by electromigration, are not the same as for neutral species; for ions, $C_j^{B_{k'}} \rightarrow (1/2)a^3$ as $|\zeta| \rightarrow 0$, however.

With co-linear forcing and bulk electroneutrality, linear superposition gives far-field decays

$$\psi' \rightarrow (1/r^2) \left[ED^E + \sum_{k=1}^M B_k D^{B_k} + UD^U \right] (\mathbf{e}_z \cdot \mathbf{e}_r) \text{ as } r \rightarrow \infty, \quad (2.48)$$

$$n'_j \rightarrow (1/r^2) \left[EC_j^E + \sum_{k=1}^M B_k C_j^{B_k} + UC_j^U \right] (\mathbf{e}_z \cdot \mathbf{e}_r) \text{ as } r \rightarrow \infty, \quad (2.49)$$

$$\begin{aligned} \mathbf{u}' \rightarrow & -(2/r^3) \left[EC^E + \sum_{k=1}^M B_k C^{B_k} + UC^U \right] (\mathbf{e}_z \cdot \mathbf{e}_r) \mathbf{e}_r \\ & - (1/r^3) \left[EC^E + \sum_{k=1}^M B_k C^{B_k} + UC^U \right] (\mathbf{e}_z \cdot \mathbf{e}_\theta) \mathbf{e}_\theta \text{ as } r \rightarrow \infty. \end{aligned} \quad (2.50)$$

This work is primarily concerned with situations where only one $X \in \{E, B_j, U\}$ is applied. Following O'Brien & White (1978), these are referred to as the (E), (B) and (U) (microscale) problems. Algebraic or differential relationships between the averaged fields may be applied to ensure zero average current density, for example. The next section relates (microscale) \mathbf{E} , \mathbf{B}_j and \mathbf{U} to the averaged (macroscale) fields, e.g. $-\langle \nabla \psi \rangle$, $\langle \nabla n_j \rangle$ and $\langle \mathbf{u} \rangle$, in dilute composites.

2.3. Averaged (bulk) fluxes

Here we calculate the average flux of the j th species

$$\langle \mathbf{j}_j \rangle = V^{-1} \int \mathbf{j}_j \, dV, \quad (2.51)$$

where the volume of integration includes the continuous and discrete phases. If the size of the representative elementary volume is between the micro- and macroscales, the result is equivalent to sampling the flux (at a point) over all micro-structural configurations (ensemble average).

Following Saville (1979) and O'Brien (1981), the averaging can be accomplished by adding and subtracting the flux

$$-D_j \nabla n_j - z_j e \frac{D_j}{kT} n_j^\infty \nabla \psi + n_j^\infty \mathbf{u} \quad (2.52)$$

from the integrand in (2.51). This yields the macroscopic electromigrative, diffusive and convective fluxes in the absence of inclusions, plus an integral whose integrand is exponentially small beyond the diffuse double layers, i.e.

$$\begin{aligned} \langle \mathbf{j}_j \rangle = & -z_j e \frac{D_j}{kT} n_j^\infty \langle \nabla \psi \rangle - D_j \langle \nabla n_j \rangle + n_j^\infty \langle \mathbf{u} \rangle \\ & + V^{-1} \int \left[z_j e \frac{D_j}{kT} n_j^\infty \nabla \psi + D_j \nabla n_j - n_j^\infty \mathbf{u} + \mathbf{j}_j \right] dV. \end{aligned} \quad (2.53)$$

Applying the divergence theorem[†] and noting that $\nabla \cdot \mathbf{j}_j = 0$, the volume integral in (2.53) becomes

[†] Note also that $\int_V \boldsymbol{\alpha} \, dV = \int_A \mathbf{x} \boldsymbol{\alpha} \cdot \hat{\mathbf{n}} \, dA - \int_V \mathbf{x} \nabla \cdot \boldsymbol{\alpha} \, dV$, where $\boldsymbol{\alpha}$ represents an arbitrary vector field.

$$\int z_j e \frac{D_j}{kT} n_j^\infty \psi \hat{\mathbf{n}} \, dA - \int z_j e \frac{D_j}{kT} n_j (\nabla \psi \cdot \hat{\mathbf{n}}) \mathbf{r} \, dA + \int D_j n_j \hat{\mathbf{n}} \, dA - \int D_j (\nabla n_j \cdot \hat{\mathbf{n}}) \mathbf{r} \, dA + \int (n_j - n_j^\infty) (\mathbf{u} \cdot \hat{\mathbf{n}}) \mathbf{r} \, dA, \quad (2.54)$$

where the surface integrals enclose the inclusions and their respective equilibrium double layer, with $\hat{\mathbf{n}}$ directed outward, into the fluid.

For dilute composites, i.e. when $n(4/3)\pi(a + \kappa^{-1})^3 \ll 1$, the integral over a representative volume V equals nV integrals with a single particle at $\mathbf{r} = \mathbf{0}$, each with $\hat{\mathbf{n}} = \mathbf{e}_r$. Therefore, noting that $n_j^0 - n_j^\infty$ is exponentially small as $r \rightarrow \infty$, and that n_j' and $\mathbf{B}_j \cdot \mathbf{r}$ are odd functions of position, the fluxes become

$$\langle \mathbf{j}_j \rangle \approx n_j^\infty \langle \mathbf{u} \rangle - z_j e \frac{D_j}{kT} n_j^\infty \langle \nabla \psi \rangle - D_j \langle \nabla n_j \rangle + n z_j e \frac{D_j}{kT} n_j^\infty \int_{r \rightarrow \infty} [\psi' - (\nabla \psi' \cdot \mathbf{r})] \mathbf{e}_r \, dA + n D_j \int_{r \rightarrow \infty} [n_j' - (\nabla n_j' \cdot \mathbf{r})] \mathbf{e}_r \, dA. \quad (2.55)$$

On superposing solutions of the independent single-particle problems, the microscale electromigrative and diffusive contributions to the average flux, i.e. the last two terms in (2.55), are

$$n z_j e \frac{D_j}{kT} n_j^\infty \int_{r \rightarrow \infty} [\psi' - (\nabla \psi' \cdot \mathbf{r})] \mathbf{e}_r \, dA = n 4 \pi z_j e \frac{D_j}{kT} n_j^\infty \left[\mathbf{E} D^E + \sum_{k=1}^M \mathbf{B}_k D^{B_k} + \mathbf{U} D^U \right], \quad (2.56)$$

and

$$n D_j \int_{r \rightarrow \infty} [n_j' - (\nabla n_j' \cdot \mathbf{r})] \mathbf{e}_r \, dA = n 4 \pi D_j \left[\mathbf{E} C_j^E + \sum_{k=1}^M \mathbf{B}_k C_j^{B_k} + \mathbf{U} C_j^U \right]. \quad (2.57)$$

Note that $\mathbf{r}(\boldsymbol{\alpha} \cdot \mathbf{e}_r)$ has been written as $(\boldsymbol{\alpha} \cdot \mathbf{r}) \mathbf{e}_r$ because $\mathbf{r} = r \mathbf{e}_r$, where $\boldsymbol{\alpha}$ represents an arbitrary vector field. Substituting (2.56) and (2.57) into (2.55) gives

$$\langle \mathbf{j}_j \rangle \approx n_j^\infty \langle \mathbf{u} \rangle - z_j e \frac{D_j}{kT} n_j^\infty \langle \nabla \psi \rangle - D_j \langle \nabla n_j \rangle + n 4 \pi z_j e \frac{D_j}{kT} n_j^\infty \left[\mathbf{E} D^E + \sum_{k=1}^M \mathbf{B}_k D^{B_k} + \mathbf{U} D^U \right] + n 4 \pi D_j \left[\mathbf{E} C_j^E + \sum_{k=1}^M \mathbf{B}_k C_j^{B_k} + \mathbf{U} C_j^U \right]. \quad (2.58)$$

Note that the average fluxes are now expressed in terms of the asymptotic coefficients from at most $2 + M$ independent single-particle problems, each of which is solved 'exactly' in this work.

2.4. Averaged (bulk) momentum conservation equations

In general, an average velocity $\langle \mathbf{u} \rangle$ is produced by the application of an average pressure gradient $\langle \nabla p \rangle$, electric field $-\langle \nabla \psi \rangle$, or concentration gradients $\langle \nabla n_j \rangle$. This section relates these to the asymptotic coefficients emerging from the single-particle problem.

Averaging the fluid momentum equation gives (see the Appendix)

$$\mathbf{0} \approx -\langle \nabla p \rangle - (\eta/\ell^2) \langle \mathbf{u} \rangle + \eta \nabla^2 \langle \mathbf{u} \rangle - \langle \rho \nabla \psi \rangle - n \langle \mathbf{f}^d \rangle \quad (2.59)$$

where $\rho = \rho^0 + \rho'$ is the charge density and $\langle \mathbf{f}^d \rangle$ is the average (hydrodynamic) force exerted by the fluid on the inclusions. Note that inertia is neglected, as are hydrodynamic and electrostatic interactions; the analysis is therefore limited to small volume fractions $n(4/3)\pi(a + \kappa^{-1})^3 \ll 1$.

Similarly to the average fluxes, let us adopt the single-particle problem to evaluate $\langle \mathbf{f}^d \rangle$. For a single inclusion in an unbounded polymer gel,

$$\begin{aligned} \langle \mathbf{f}^d \rangle &\approx \int_{r=a} \left[-(\mathbf{P} \cdot \mathbf{r} + p')\mathbf{I} + 2\eta\mathbf{e} \right] \cdot \mathbf{e}_r \, dA \\ &= \int_{r \rightarrow \infty} \left[-(\mathbf{P} \cdot \mathbf{r} + p')\mathbf{I} + 2\eta\mathbf{e} \right] \cdot \mathbf{e}_r \, dA - \int_{r=a}^{\infty} \left[(\eta/\ell^2)\mathbf{u} + \rho\nabla\psi \right] dV, \end{aligned} \quad (2.60)$$

where $\mathbf{e} = (1/2)[\nabla\mathbf{u} + (\nabla\mathbf{u})^T]$ and \mathbf{I} is the identity tensor. Since $\nabla \cdot \mathbf{u} = 0$, $\mathbf{u}(r=a) = \mathbf{0}$, and $\nabla p = -(\eta/\ell^2)\mathbf{u}$, and $\mathbf{u}' \sim r^{-3}$ as $r \rightarrow \infty$, (2.60) can be written

$$\langle \mathbf{f}^d \rangle \approx - \int_{r \rightarrow \infty} [p' - (\nabla p' \cdot \mathbf{r})]\mathbf{e}_r \, dA - \int_{r=a}^{\infty} \rho\nabla\psi \, dV. \quad (2.61)$$

Beyond the double layer,

$$p' = -(\eta/\ell^2) \int_r^{\infty} (2/r'^3)C^X(\mathbf{X} \cdot \mathbf{e}_r) \, dr' = -(1/r^2)(\eta/\ell^2)C^X(\mathbf{X} \cdot \mathbf{e}_r), \quad (2.62)$$

and because the integrand of the volume integral in (2.61) is exponentially small there,

$$\langle \rho\nabla\psi \rangle \approx n \int_{r=a}^{\infty} \rho\nabla\psi \, dV. \quad (2.63)$$

Therefore,

$$\langle \mathbf{f}^d \rangle \approx (\eta/\ell^2)4\pi \left[\mathbf{E}C^E + \sum_{k=1}^M \mathbf{B}_k C^{B_k} + \mathbf{U}C^U \right] - n^{-1}\langle \rho\nabla\psi \rangle \quad (2.64)$$

and, hence, (2.59) becomes

$$\mathbf{0} \approx -\langle \nabla p \rangle - (\eta/\ell^2)\langle \mathbf{u} \rangle + \eta\nabla^2\langle \mathbf{u} \rangle - n(\eta/\ell^2)4\pi \left[\mathbf{E}C^E + \sum_{k=1}^M \mathbf{B}_k C^{B_k} + \mathbf{U}C^U \right]. \quad (2.65)$$

Note that, in addition to $\langle \mathbf{f}^d \rangle$, an electrical force $\langle \mathbf{f}^e \rangle$ and a mechanical-contact force $\langle \mathbf{f}^m \rangle$ act on the inclusions. Accordingly, static equilibrium requires

$$\begin{aligned} \langle \mathbf{f}^m \rangle &= -\langle \mathbf{f}^e \rangle - \langle \mathbf{f}^d \rangle \\ &\approx -(\eta/\ell^2)4\pi \left[\mathbf{E}C^E + \sum_{k=1}^M \mathbf{B}_k C^{B_k} + \mathbf{U}C^U \right]. \end{aligned} \quad (2.66)$$

In the absence of charge, for example, $-\langle \mathbf{f}^m \rangle$ is equal to the drag force on a sphere embedded in a Brinkman medium with viscosity η and Darcy permeability ℓ^2 . Indeed, Brinkman (1947) solved this problem exactly, obtaining

$$\langle \mathbf{f}^m \rangle = -2\pi\eta\mathbf{U}a(\ell/a)^2[1 + 3(\ell/a) + 3(\ell/a)^2] \quad (\zeta = 0, \phi \rightarrow 0), \quad (2.67)$$

which shows that

$$2C^U/a^3 = 1 + 3(\ell/a) + 3(\ell/a)^2 \quad (\zeta = 0, \phi \rightarrow 0). \quad (2.68)$$

Note that the drag force approaches the Stokes drag $6\pi\eta aU$ as $\ell/a \rightarrow \infty$. When $\ell/a \rightarrow 0$, however, the drag approaches $2\pi a^3(\eta/\ell^2)U$ because the surface traction is dominated by the pressure (dipole) arising from the outer Darcy flow: $\nabla^2 p' = 0$ with $\mathbf{u} = -(\ell^2/\eta)\nabla p'$.

2.5. Averaged (bulk) equations for unidirectional transport

With all average fluxes in the z -direction, mass and momentum conservation require constant $\langle \mathbf{u} \rangle$ and, hence,

$$\langle \nabla p \rangle = -(\eta/\ell^2)\langle \mathbf{u} \rangle - \phi(3/a^3)(\eta/\ell^2) \left[\mathbf{E}C^E + \sum_{k=1}^M \mathbf{B}_k C^{B_k} + \mathbf{U}C^U \right]. \quad (2.69)$$

Similarly, the (steady) average species conservation equations $\nabla \cdot \langle \mathbf{j}_j \rangle = 0$ require constant average fluxes

$$\begin{aligned} \langle \mathbf{j}_j \rangle &= n_j^\infty \langle \mathbf{u} \rangle - z_j e \frac{D_j}{kT} n_j^\infty \langle \nabla \psi \rangle - D_j \langle \nabla n_j \rangle \\ &+ \phi(3/a^3) z_j e \frac{D_j}{kT} n_j^\infty \left[\mathbf{E}D^E + \sum_{k=1}^M \mathbf{B}_k D^{B_k} + \mathbf{U}D^U \right] \\ &+ \phi(3/a^3) D_j \left[\mathbf{E}C_j^E + \sum_{k=1}^M \mathbf{B}_k C_j^{B_k} + \mathbf{U}C_j^U \right]. \end{aligned} \quad (2.70)$$

Note that $\nabla \cdot \langle \nabla \psi \rangle = 0$ in an electrically neutral composite with uniform dielectric permittivity, so the average electric field is also constant.

The averages can be expanded as power series in the inclusion volume fraction, e.g. $\langle \mathbf{u} \rangle \rightarrow \mathbf{U}_0 + \phi \mathbf{U}_1 + O(\phi^2)$. Therefore, since the microscale equations (asymptotic coefficients) are accurate to $O(\phi)$, the notation is condensed by writing, for example, $\langle \mathbf{u} \rangle \equiv \mathbf{U}$, where it is understood that $\mathbf{U} = \mathbf{U}_0 + \phi \mathbf{U}_1 + O(\phi^2)$. Clearly, \mathbf{E} , \mathbf{B}_j and \mathbf{U} in (2.69) and (2.70) need only to include the $O(1)$ contribution to their respective average, e.g. $\mathbf{U} \rightarrow \mathbf{U}_0$. The following notation is adopted for the other averaged quantities: $\mathbf{J}_j \equiv \langle \mathbf{j}_j \rangle$, $\mathbf{P} \equiv \langle \nabla p \rangle$, $\mathbf{B}_j \equiv \langle \nabla n_j \rangle$, $\mathbf{E} \equiv -\langle \nabla \psi \rangle$.

With one electrolyte ($M=1$) and, recall, bulk electroneutrality, there are $N+4$ independent variables (\mathbf{E} , \mathbf{U} , \mathbf{P} , \mathbf{B}_k ($k=1$), \mathbf{J}_j ($j=1, \dots, N$)) with $N+1$ independent equations (see (2.69) and (2.70)). Clearly, three independent variables must be specified for a unique solution.

For clarity, the results presented below involve a 1-1 electrolyte (NaCl), mostly with only one non-zero forcing variable. It is important to note that, because the equations are linear, solutions for any combination of forcing variables may be constructed. For example, a companion paper (Hill 2006) establishes the electric field strength required to maintain a constant electrolyte flux – driven by a bulk concentration gradient across a membrane – with zero bulk current density.

3. Response to an electric field

Results are now presented for the application of an electric field in the absence of average pressure and concentration gradients. These conditions prevail when measuring the electrical conductivity, for example, and they provide a relatively simple setting in which to study the influence of inclusions on bulk electrokinetic transport. Steady homogeneous conditions are assumed, neglecting the influence of

$\zeta e/(kT)$	D^E/a^3	$C_j^E kT/(2Ia^3 e)$ ($j=1, 2$)	$C^E kT/(u^* a^4 e)$	$U/(E\phi) = -3C^E/a^3$ ($(\text{nm s}^{-1})/(\text{V cm}^{-1})$)
$\kappa a = 1$ $I = 9.25 \times 10^{-6} \text{ mol l}^{-1}$				
-1	-3.82×10^{-1}	1.04	-1.87×10^{-4}	1.13
-2	-5.71×10^{-2}	2.04	-3.66×10^{-4}	2.20
-4	8.66×10^{-1}	3.72	-6.64×10^{-4}	3.99
-6	1.60	4.77	-8.40×10^{-4}	5.05
-8	1.96	5.28	-9.04×10^{-4}	5.44
$\kappa a = 10$ $I = 9.25 \times 10^{-4} \text{ mol l}^{-1}$				
-1	-4.74×10^{-1}	7.30×10^{-2}	-1.20×10^{-3}	7.22
-2	-3.98×10^{-1}	1.51×10^{-1}	-2.42×10^{-3}	1.46×10^1
-4	-1.37×10^{-1}	3.24×10^{-1}	-4.63×10^{-3}	2.78×10^1
-6	1.32×10^{-1}	4.76×10^{-1}	-5.45×10^{-3}	3.28×10^1
-8	2.95×10^{-1}	5.64×10^{-1}	-4.70×10^{-3}	2.83×10^1
$\kappa a = 100$ $I = 9.25 \times 10^{-2} \text{ mol l}^{-1}$				
-1	-4.96×10^{-1}	7.83×10^{-3}	-6.97×10^{-3}	4.19×10^1
-2	-4.82×10^{-1}	1.79×10^{-2}	-1.42×10^{-2}	8.51×10^1
-4	-4.11×10^{-1}	5.58×10^{-2}	-2.87×10^{-2}	1.73×10^2
-6	-2.53×10^{-1}	1.35×10^{-1}	-3.83×10^{-2}	2.30×10^2
-8	-3.81×10^{-2}	2.43×10^{-1}	-3.58×10^{-2}	2.15×10^2

TABLE 1. Dimensionless asymptotic coefficients (equation (3.2)) and incremental pore mobility (equation (3.3)) for bulk electromigration of NaCl in a Brinkman medium with charged spherical inclusions: $a = 100 \text{ nm}$; $\ell \approx 0.951 \text{ nm}$; $T = 25^\circ\text{C}$; $D_1 \approx 1.33 \times 10^{-9} \text{ m}^2 \text{ s}^{-1}$ (Na^+); $D_2 \approx 2.03 \times 10^{-9} \text{ m}^2 \text{ s}^{-1}$ (Cl^-); $u^* = \epsilon_s \epsilon_o (kT/e)^2 / (\eta a) \approx 5.15 \times 10^{-3} \text{ m s}^{-1}$.

electrode polarization and electrochemical reactions. Accordingly, the average velocity from (2.69) is

$$U = -\phi(3/a^3)EC^E + O(\phi^2), \quad (3.1)$$

and the average ion fluxes from (2.70) are

$$\begin{aligned} \mathbf{J}_j = & z_j e \frac{D_j}{kT} n_j^\infty \mathbf{E} + \phi(3/a^3) z_j e \frac{D_j}{kT} n_j^\infty \mathbf{E} D^E \\ & + \phi(3/a^3) D_j \mathbf{E} C_j^E + \phi(3/a^3) n_j^\infty \mathbf{E} C^E + O(\phi^2). \end{aligned} \quad (3.2)$$

Asymptotic coefficients are provided in table 1 for a composite with Brinkman screening length $\ell \approx 0.951 \text{ nm}$ and inclusion radius $a = 100 \text{ nm}$; the ζ -potentials and (three) ionic strengths span experimentally accessible ranges. With a positive electric field ($E > 0$), the counter-ions (Na^+) migrate toward the ‘front’ of the inclusions, inducing a positive electrostatic dipole moment $D^E > 0$. When the ζ -potential is low, however, the dipole moment reflects the dielectric polarization required to maintain an impenetrable interface, so the dipole strength approaches the Maxwell value $D^E = -(1/2)a^3$ (for non-conducting spheres) as $|\zeta| \rightarrow 0$. The positive concentration dipole moments $C_j^E > 0$ reflect the combined influences of electromigration, diffusion, and electroneutrality. As expected from (2.47), $C^E < 0$, because the electrical force on the fluid and, hence, the resulting electro-osmotic flow are forward ($U > 0$).

3.1. Incremental pore velocity

As suggested by (3.1), the ratio

$$U/(E\phi) = -3C^E/a^3, \quad (3.3)$$

which is termed the *incremental pore mobility*, provides a convenient measure of the electro-osmotic pumping capacity. When multiplied by the electric field strength and particle volume fraction, the values in the last column of table 1, for example, yield the $O(\phi)$ average velocity that prevails in the absence of an applied pressure gradient. This section examines how the strength of the flow is related to the ζ -potential and size of the inclusions, the ionic strength of the electrolyte, and the permeability of the gel. We will see that the pore mobility is significantly influenced by polarization and relaxation, so the qualitative form of the relationship (with a given gel permeability) is similar to the classical electrophoretic mobility of dispersions (O'Brien & White 1978).

Consider the case in table 1 with $\kappa a = 100$ and $\zeta = -1kT/e$. With $E = 2 \text{ V cm}^{-1}$ and $\phi = 10^{-2}$, the pore velocity is $U \approx 0.84 \text{ nm s}^{-1}$, which is clearly very slow. If, however, this flow is directed from a composite with a 1 cm^2 cross-section into a microfluidic channel, then it is not unreasonable to amplify the velocity by four orders of magnitude, yielding a (modest) average velocity of $8.4 \text{ } \mu\text{m s}^{-1}$. In this example, the permeability ($\ell^2 = 0.951^2 \text{ nm}^2$) is relatively low, so higher velocities may be achieved with a comparable (weak) electric field and inclusion volume fraction. Note that a stronger electric field between (platinum) electrodes separated by a distance $L \sim 5 \text{ mm}$, say, produces hydrogen and oxygen bubbles. In conventional electro-osmotic pumps, much higher electric field strengths are achieved by catalytically recombining hydrogen and oxygen (Yao *et al.* 2003). For the purpose of accurately determining the pore mobility, however, higher electric field strengths are, perhaps, unnecessary.

The pore mobility is shown in figure 3(a) as a function of the ζ -potential for various values of κa , with inclusion radii $a = 10, 100$ and 1000 nm (top-to-bottom panels), and Brinkman screening length $\ell \approx 3.11 \text{ nm}$. Similarly to the electrophoretic mobility (e.g. O'Brien & White 1978), at low to moderate ζ -potentials the pore mobility provides a one-to-one connection between the (measured) pore velocity and the surface charge. Mobility maxima arise from polarization (by electromigration) and relaxation (by diffusion) of the equilibrium double layer. As suggested by earlier theoretical studies examining the role of polarization and relaxation on the electrophoretic mobility of polymer-coated particles (Saville 2000; Hill 2004; Hill & Saville 2005), these calculations clearly demonstrate that polarization is driven by electromigration, since convection is extremely weak when the particles are immobilized in a polymer gel. Note that theoretical studies of electro-osmotic flow in micro-porous membranes do not reveal such maxima, because the underlying microscale model comprises (effectively) straight channels with charged walls (Yao & Santiago 2003).

As expected, the (incremental) pore mobility tends to increase with ζ -potential at fixed ionic strength, and increases with ionic strength at fixed ζ -potential. Both trends reflect the increasing charge required to maintain a constant surface potential when varying the ionic strength. For colloids whose surface charge is independent of electrolyte concentration, the ζ -potential increases with decreasing κa . Accurate semi-empirical expressions for this relationship (obtained from solutions of the Poisson–Boltzmann equation) are readily available (Russel *et al.* 1989). In general, however, the dependence of surface charge density on ionic strength and pH is exceedingly difficult to predict, and must therefore be determined empirically for specific interfaces (e.g. see Yao *et al.* 2003, for silica in the presence of KCl).

For a closer connection to experiments, the pore mobility is shown in figure 3(b) as a function of the ionic strength with three constant surface charge densities spanning two orders of magnitude. Note that the inclusion radii are the same as in the corresponding panels in (a). Because the surface charge is fixed, the ζ -potential

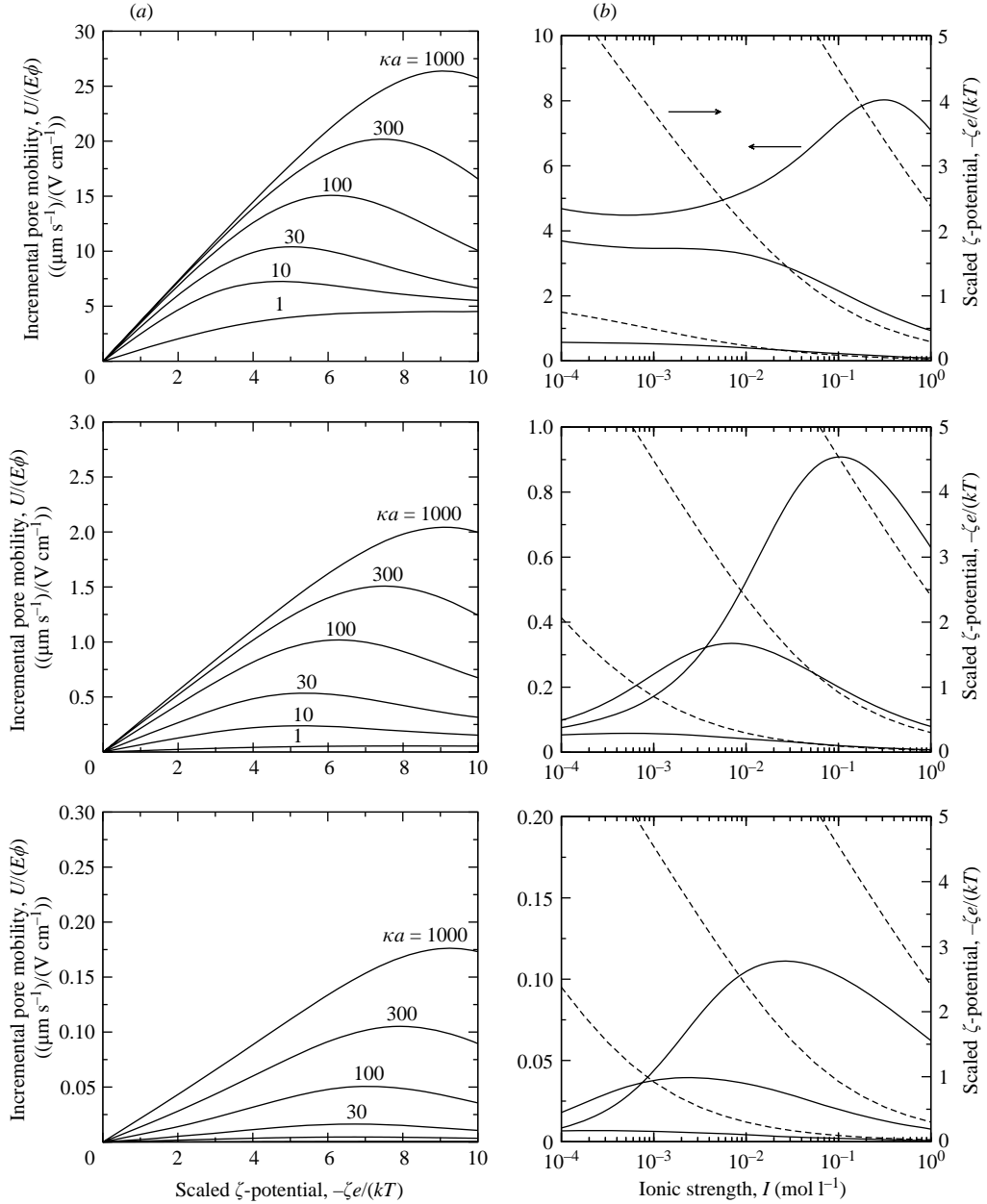


FIGURE 3. The incremental pore mobility $U/(E\phi)$ with inclusion radii $a = 10$ (top), 100 (middle) and 1000 nm (bottom): aqueous NaCl at $T = 25^\circ\text{C}$; $\ell \approx 3.11$ nm. (a) The mobility as a function of the (scaled) ζ -potential $\zeta e/(kT)$ for various (scaled) reciprocal double-layer thicknesses $\kappa a = 1, 10, 30, 100, 300$ and 1000 . (b) The mobility (solid lines, left axis) and ζ -potential (dashed lines, right axis) as a function of the ionic strength with constant surface charge densities $-\sigma \approx 0.179, 1.79$ and $17.9 \mu\text{C cm}^{-2}$ (increasing upward at high ionic strength).

(dashed lines, right axis) decreases with increasing ionic strength, but the particle size does not significantly influence the ζ -potential. Because the average velocity reflects the combined influence of all particles in the composite, U is expected to be proportional to the $O(n\sigma a^2 \sim \sigma\phi/a)$ (average) counter-charge density. Therefore,

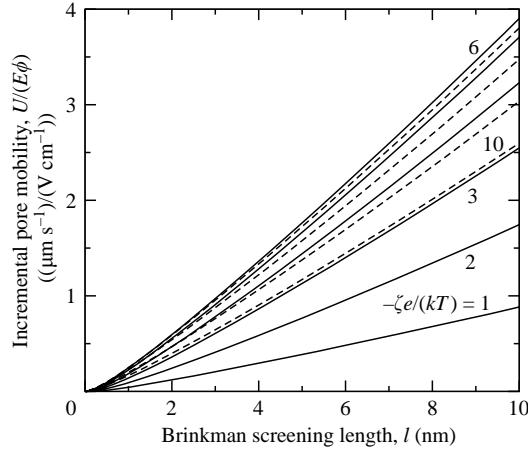


FIGURE 4. The incremental pore mobility $U/(E\phi)$ as a function of the Brinkman screening length ℓ for various (scaled) ζ -potentials $-\zeta e/(kT) = 1, 2, 3, \dots, 6$ (solid lines) $7, \dots, 10$ (dashed lines): aqueous NaCl at $T = 25^\circ\text{C}$; $a = 100\text{ nm}$; $\kappa a = 100$ ($I \approx 0.0925\text{ mol l}^{-1}$). An electric field is applied in the absence of average pressure and concentration gradients. The maximum velocity is achieved when $|\zeta|e/(kT) \approx 6$.

balancing the corresponding $O(E\sigma\phi/a)$ electrical force with the $O(\eta U/\ell^2)$ Darcy drag force gives a pore mobility $U/(\phi E) \sim \sigma\ell^2/(\eta a)$. Indeed, comparing the mobility axes (left sides) of figure 3(b) indicates that the mobility is, at least approximately, inversely proportional to the inclusion radius. Again, at low ionic strengths, when the ζ -potential is high, polarization and relaxation significantly complicate this simple interpretation.

To highlight the influence of polymer-gel permeability, the pore mobility is shown in figure 4 as a function of the Brinkman screening length ℓ for various ζ -potentials. With a particle radius $a = 100\text{ nm}$, the ionic strength $I \approx 0.0925\text{ mol l}^{-1}$ yields $\kappa a = 100$ and $\kappa\ell > 1$ at most values of ℓ . Now the mobility increases as ℓ^m with exponent $m(\ell)$ in the range 1–2, indicating that viscous stresses and Darcy drag balance the electrical body force. Note that the mobility increases linearly with the ζ -potential when $|\zeta|$ is small, and, again, mobility maxima are evident when $|\zeta| \approx 6kT/e$. Pore mobilities are shown in figure 5 at a much lower ionic strength $I \approx 9.25 \times 10^{-6}\text{ mol l}^{-1}$ yielding $\kappa a = 1$. Now, as expected, the mobility increases linearly with ℓ^2 , since $\kappa\ell < 1$. The monotonic increase with ζ -potential is because the surface charge densities are low and, hence, polarization is weak.

3.2. Electro-osmotic pumping

Recall that the (incremental) pore mobility was defined with zero average pressure gradient, and therefore neglects the pressure differential $\Delta p = PL$ required to pump fluid through an external network. This section briefly addresses coupling the composite and electrodes – which together are referred to as an electro-osmotic pump – to a microfluidic network. The analysis briefly considers the force exerted on the composite, electrical power consumption, and pump efficiency.

Let us consider a closed loop, where fluid in the composite exits from one side, passes through a microfluidic network, and returns to the other side. To ensure that all electrical current flows through the composite, we assume that the electrical resistance of the network is much greater than that of the pump, which is realized when the

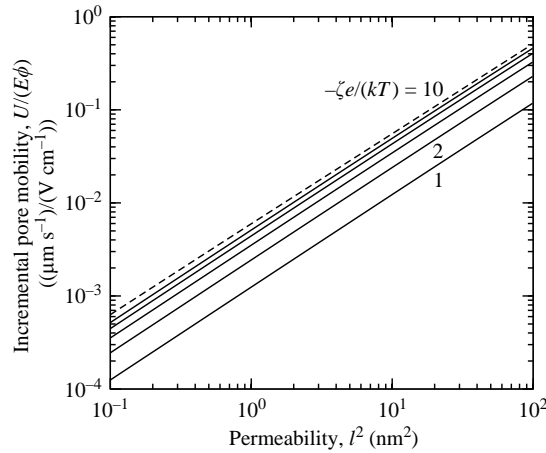


FIGURE 5. The incremental pore mobility $U/(E\phi)$ as a function of the Darcy permeability ℓ^2 for various (scaled) ζ -potentials $-\zeta e/(kT) = 1, 2, 3, \dots, 6$ (solid lines) 10 (dashed line): aqueous NaCl at $T = 25^\circ\text{C}$; $a = 100$ nm; $\kappa a = 1$ ($I \approx 9.25 \times 10^{-6}$ mol l^{-1}).

length (area) of the external network L_e (d^2) is much greater (smaller) than that of the composite L (A). Next, assuming laminar viscous flow, the pressure drop through the network may be written

$$\Delta p \approx \eta c (L_e/d^4) Q, \quad (3.4)$$

where d^2 is the (characteristic) channel cross-sectional area, Q is the volumetric flow rate, and c is an $O(1)$ constant that reflects the shape and length the network sections.

Equating the network pressure drop to the pump characteristic emerging from (2.65),

$$\Delta p/L = -(\eta/\ell^2)U - \phi(3/a^3)(\eta/\ell^2)(EC^E + UC^U), \quad (3.5)$$

gives

$$[\eta c (L_e/d^4)(A/L) + (\eta/\ell^2) + \phi(3/a^3)(\eta/\ell^2)C^U]Q/A = -\phi(3/a^3)(\eta/\ell^2)EC^E, \quad (3.6)$$

where A and L are the composite cross-sectional area and length.

The contribution of the back-flow, as represented by the asymptotic coefficient C^U in (3.6), is obtained from the (U) problem. This and other asymptotic coefficients are provided in table 2 for a composite with Brinkman screening length $\ell \approx 0.951$ nm and inclusion radius $a = 100$ nm; again, the ζ -potentials and (three) ionic strengths span experimentally accessible ranges. Here, the average force exerted by the polymer on the inclusions $\langle f^m \rangle = -4\pi(\eta/\ell^2)C^U U$ (equation (2.66)) is independent of the surface charge. Note that $C^U = (1/2)a^3$ when the only contribution to the force is due to Darcy flow ($\ell/a \ll 1$); the (constant) value $C^U/a^3 \approx 0.514$ in table 2, which reflects a small viscous contribution ($\ell/a = 0.00951$), is precisely the value given by Brinkman's theory (equation (2.67)). The flow-induced electrical and concentration polarization, as represented by D^U and C_j^U , are related to the streaming potential and streaming current, and are included here only for future reference.

When the dominant resistance comes from the composite itself (the second term on the left-hand side of (3.6)), the pump performance curve simplifies to

$$Q \approx -\phi(3/a^3)AEC^E, \quad (3.7)$$

$\zeta e/(kT)$	$D^U eu^*/(kTa^2)$	$C_j^U u^*/(2Ia^2)$ ($j = 1, 2$)	C^U/a^3
	$\kappa a = 1$	$I = 9.25 \times 10^{-6} \text{ mol l}^{-1}$	
-1	6.70×10^{-1}	8.71×10^{-2}	5.14×10^{-1}
-2	1.32	2.03×10^{-1}	5.14×10^{-1}
-4	2.44	4.49×10^{-1}	5.14×10^{-1}
-6	3.10	6.06×10^{-1}	5.14×10^{-1}
-8	3.33	6.44×10^{-1}	5.14×10^{-1}
	$\kappa a = 10$	$I = 9.25 \times 10^{-4} \text{ mol l}^{-1}$	
-1	4.38×10^{-2}	7.76×10^{-4}	5.14×10^{-1}
-2	9.10×10^{-2}	2.16×10^{-3}	5.14×10^{-1}
-4	1.81×10^{-1}	5.58×10^{-3}	5.14×10^{-1}
-6	2.19×10^{-1}	7.08×10^{-3}	5.14×10^{-1}
-8	1.96×10^{-1}	5.74×10^{-3}	5.14×10^{-1}
	$\kappa a = 100$	$I = 9.25 \times 10^{-2} \text{ mol l}^{-1}$	
-1	2.55×10^{-3}	4.49×10^{-6}	5.14×10^{-1}
-2	5.33×10^{-3}	1.27×10^{-5}	5.14×10^{-1}
-4	1.14×10^{-2}	3.69×10^{-5}	5.14×10^{-1}
-6	1.64×10^{-2}	5.93×10^{-5}	5.14×10^{-1}
-8	1.70×10^{-2}	6.14×10^{-5}	5.14×10^{-1}

TABLE 2. Dimensionless asymptotic coefficients for bulk convection of NaCl in a Brinkman medium with charged spherical inclusions: $a = 100 \text{ nm}$; $\ell \approx 0.951 \text{ nm}$; $T = 25^\circ\text{C}$, $D_1 \approx 1.33 \times 10^{-9} \text{ m}^2 \text{ s}^{-1}$ (Na^+); $D_2 \approx 2.03 \times 10^{-9} \text{ m}^2 \text{ s}^{-1}$ (Cl^-); $u^* \approx 5.15 \times 10^{-3} \text{ m s}^{-1}$.

which is clearly independent of the applied load. Neglecting constraints imposed by electrolysis, for example, the maximum length of the composite may be set by consideration of the electrical power consumption

$$\mathcal{P} \approx K^\infty E^2 AL + O(\phi). \tag{3.8}$$

Note that the force exerted on the composite

$$F = -\Delta p A \approx \eta c (L_e/d^4) A^2 \phi (3/a^3) EC^E \tag{3.9}$$

reflects the pressure required to pump fluid through the network. Therefore, the average shear stress $\tau \sim -F/(L\sqrt{A})$ required to support the composite scales as

$$\tau \sim -\eta c (L_e/d^4) (A^{3/2}/L) \phi (3/a^3) EC^E. \tag{3.10}$$

Since the area A will be set by the flow rate, the length of the composite should be set by the maximum allowable shear stress.

Finally, the pump efficiency, as measured by the ratio of the rate of flow work $|Q\Delta p|$ to the electrical power consumption \mathcal{P} is

$$\mathcal{E} \approx \eta c (L_e/d^4) [\phi (3/a^3) C^E]^2 A / (K^\infty L). \tag{3.11}$$

Because C^E depends on ζ , κa , ℓ , etc., care must be taken in interpreting this equation. Nevertheless, geometrical considerations alone clearly favour thin membranes with large cross-sectional area, operating with a low ionic strength (conductivity) and a high inclusion volume fraction. In practice, an optimal design (with specified flow Q and, perhaps, voltage $V = \Delta\psi$) will be constrained by consideration of the mechanical strength of the composite (as indicated by (3.9) and (3.10)), which clearly diminishes with decreasing thickness L and increasing area A .

3.3. Incremental pressure gradient

Now consider the pressure gradient produced by an average electric field with zero average flow. This situation may be realized when an electrolyte-saturated composite is bounded by a vessel with impenetrable walls. A practical application involves measuring the differential (static) pressure Δp to infer the permeability of the polymer gel or, for example, the ζ -potential of the inclusions. Note that zero average flow does not imply stationary fluid at the microscale, because the ‘inner’ electro-osmotic flow around each inclusion is balanced by a far-field pressure-driven back-flow, analogous to the situation encountered in microelectrophoresis capillaries with blocked ends.

Setting $U = 0$ in (2.69) gives

$$\mathbf{P} = -\phi(\eta/\ell^2)(3/a^3)C^E \mathbf{E} + O(\phi^2), \quad (3.12)$$

which is termed the *incremental pressure gradient*. Representative values may be calculated by multiplying the incremental pore mobilities in the last column of table 1, and plotted in figures 3–5, by their respective values of η/ℓ^2 .

It is interesting to note that when $\kappa\ell < 1$ and, hence, the pore mobility increases linearly with ℓ^2 (see figure 5), the pressure gradient is independent of the permeability. This is because increasing the permeability increases the electric-field-induced flow, and, since the back-flow and accompanying pressure gradient are proportional to each other, it follows that the pressure gradient is independent of ℓ^2 . However, at higher ionic strengths, when $\kappa\ell > 1$ (see figure 4), the pressure gradient evidently decreases with ℓ^2 . This is because the electric-field-induced flow within the diffuse double layers – where resistance to flow is predominantly due to viscous stress – increases more slowly with the permeability than the Darcy drag beyond the double layers decreases.

Note that the incremental pressure gradient reflects the same asymptotic coefficient C^E as the pore mobility, so it is important to establish whether measuring the electric-field-induced pressure gradient offers a significant advantage over measuring the pore mobility. Recall that pore mobilities can generate low but measurable velocities in a microchannel. From table 1 with $\kappa a = 100$ and $\zeta = -1kT/e$, setting $E = 2 \text{ V cm}^{-1}$ and $\phi = 10^{-2}$ yields $P \approx 8.76 \text{ kPa cm}^{-1}$. Therefore, when $L = 5 \text{ mm}$, for example, the pressure differential is $|\Delta p| \approx 4.38 \text{ kPa}$ (static head of 0.43 m of water). Clearly, the pressure gradient induced by a relatively weak electric field is sufficient to produce a modest (static) pressure.

3.4. Species fluxes

Let us write the average flux of each species from (3.2) as

$$\mathbf{J}_j = z_j e \frac{D_j}{kT} n_j^\infty \mathbf{E} (1 + \phi \Delta_j^E), \quad (3.13)$$

where

$$\begin{aligned} \Delta_j^E &= \Delta_{j,e}^E + \Delta_{j,d}^E + \Delta_{j,c}^E \\ &= (3/a^3)D^E + (3/a^3) \frac{kT}{z_j e n_j^\infty} C_j^E + (3/a^3) \frac{kT}{z_j e D_j} C^E \end{aligned} \quad (3.14)$$

is the sum of incremental microscale contributions (of electromigration, diffusion, and convection, respectively) to the average electromigrative flux.

The ratio of the convective and electromigrative terms is

$$\Delta_{j,c}^E / \Delta_{j,e}^E = \frac{C^E}{z_j e (D_j/kT) D^E} \sim P e_j / z_j, \quad (3.15)$$

and the ratio of the convective and diffusive terms is

$$\Delta_{j,c}^E/\Delta_{j,d}^E = \frac{n_j^\infty C^E}{D_j C_j^E} \sim Pe_j, \quad (3.16)$$

where the Péclet number $Pe_j = u_c \kappa^{-1}/D_j$ is typically very small. The characteristic (microscale) velocity u_c may be estimated by balancing the $O(E\sigma\kappa)$ electrical force (per unit volume) with the $O(u_c\eta/\ell^2)$ Darcy drag force, giving $u_c \sim E\sigma\kappa\ell^2/\eta$. With $E \sim 10^2 \text{ V cm}^{-1}$, $\sigma \sim 1 \text{ } \mu\text{C cm}^{-2}$, $\kappa^{-1} \sim 10^2 \text{ nm}$, $\ell \sim 1 \text{ nm}$, and $\eta \sim 10^{-3} \text{ kg m}^{-1}\text{s}^{-1}$, $u_c \sim 1 \text{ } \mu\text{m s}^{-1}$. Further, with $a \sim 1 \text{ } \mu\text{m}$ and $D_j \sim 10^{-9} \text{ m}^2 \text{ s}^{-1}$, $Pe_j \sim 10^{-4}$, indicating that diffusion and electromigration ($z_j \neq 0$) dominate convection. Clearly, for charged species with $z_j \sim 1$, electromigrative fluxes are comparable to diffusive fluxes.

Incremental contributions to the ion fluxes are provided in table 3 for the composite whose asymptotic coefficients are shown in table 1. These confirm that the convective contribution $\Delta_{j,c}^E$ is small, and that the electromigrative contribution $\Delta_{j,e}^E$ approaches the Maxwell value $\Delta_{j,e}^E = -3/2$ for impenetrable (non-conducting) spheres as $|\zeta| \rightarrow 0$. Furthermore, the electromigrative ($\Delta_{j,e}^E$) and diffusive ($\Delta_{j,d}^E$) contributions for Na^+ and Cl^- vary significantly with ionic strength. For example, at low electrolyte concentration, the diffusive term dominates, enhancing the flux of the counter-ion (Na^+) and attenuating that of the co-ion (Cl^-).

3.5. Electrical conductivity

The electrical conductivity of colloidal dispersions is well known to reflect the particle surface charge density (Russel *et al.* 1989). The conductivity of a composite with immobilized particles presents a relatively simple problem when the electrolyte ions are unhindered by the polymer, because only the electrolyte ions – not the charge on the particles (macroions) themselves – contribute to charge transfer. This section establishes whether the electrical conductivity is sensitive to the surface charge and, possibly, the permeability of the polymer gel.

From the fluxes in (3.2), the average current density may be written

$$\mathbf{I} = \sum_{j=1}^N z_j e \mathbf{J}_j \approx K^\infty \mathbf{E} + \phi(3/a^3) \mathbf{E} \left[K^\infty D^E + \sum_{j=1}^N z_j e D_j C_j^E \right], \quad (3.17)$$

where

$$K^\infty = \sum_{j=1}^N (z_j e)^2 \frac{D_j}{kT} n_j^\infty \quad (3.18)$$

is the conductivity of the electrolyte. The conductivity of the composite is defined as

$$K^* = I/E = K^\infty(1 + \phi\Delta^K), \quad (3.19)$$

where Δ^K is termed the (dimensionless) *conductivity increment*.

Equations (3.17)–(3.19) are equivalent to expressions derived by O'Brien (1981) for the conductivity of dilute colloidal dispersions with the particles undergoing electrophoresis. Here, the asymptotic coefficients are different because the particles are stationary†. When the ζ -potential is low and, hence, ion fluxes are unperturbed by the surface charge, the dipole strength for non-conducting spheres equals the Maxwell

† When particles undergo electrophoresis in a Newtonian electrolyte, the far-field (solenoidal) velocity disturbance is irrotational, decaying as r^{-3} as $r \rightarrow \infty$. When fixed in electrolyte without polymer, however, the far-field disturbance reflects a net force, decaying as r^{-1} as $r \rightarrow \infty$.

$\zeta e/(kT)$	$\Delta_{j,e}^E (j=1,2)$	$\Delta_{1,d}^E (\text{Na}^+) (= -\Delta_{2,d}^E)$	$\Delta_{1,c}^E (\text{Na}^+)$	$\Delta_{2,c}^E (\text{Cl}^-)$	$\Delta_1^E (\text{Na}^+)$	$\Delta_2^E (\text{Cl}^-)$	Δ^K
			$\kappa a = 1$	$I = 9.25 \times 10^{-6} \text{ mol l}^{-1}$			
-1	-1.15	6.25	-2.17×10^{-4}	1.42×10^{-4}	5.10	-7.39	-2.44
-2	-1.71×10^{-1}	1.22×10^1	-4.25×10^{-4}	2.78×10^{-4}	1.21×10^1	-1.24×10^1	-2.72
-4	2.60	2.23×10^1	-7.70×10^{-4}	5.05×10^{-4}	2.49×10^1	-1.97×10^1	-2.05
-6	4.79	2.86×10^1	-9.74×10^{-3}	6.38×10^{-4}	3.34×10^1	-2.39×10^1	-1.16
-8	5.89	3.17×10^1	-1.05×10^{-3}	6.87×10^{-4}	3.76×10^1	-2.58×10^1	-6.91×10^{-1}
			$\kappa a = 10$	$I = 9.25 \times 10^{-4} \text{ mol l}^{-1}$			
-1	-1.42	4.38×10^{-1}	-1.39×10^{-3}	9.12×10^{-4}	-9.85×10^{-1}	-1.86	-1.51
-2	-1.19	9.08×10^{-1}	-2.81×10^{-3}	1.84×10^{-3}	-2.88×10^{-1}	-2.10	-1.38
-4	-4.11×10^{-1}	1.95	-5.36×10^{-3}	3.52×10^{-3}	1.53	-2.35	-8.16×10^{-1}
-6	3.96×10^{-1}	2.86	-6.32×10^{-3}	4.14×10^{-3}	3.25	-2.46	-1.98×10^{-1}
-8	8.84×10^{-1}	3.38	-5.45×10^{-3}	3.57×10^{-3}	4.26	-2.50	1.81×10^{-1}
			$\kappa a = 100$	$I = 9.25 \times 10^{-2} \text{ mol l}^{-1}$			
-1	-1.49	4.70×10^{-2}	-8.08×10^{-3}	5.30×10^{-3}	-1.45	-1.53	-1.50
-2	-1.45	1.08×10^{-1}	-1.64×10^{-2}	1.08×10^{-2}	-1.36	-1.54	-1.47
-4	-1.23	3.35×10^{-1}	-3.33×10^{-2}	2.18×10^{-2}	-9.31×10^{-1}	-1.55	-1.30
-6	-7.59×10^{-1}	8.11×10^{-1}	-4.44×10^{-2}	2.91×10^{-2}	7.38×10^{-3}	-1.54	-9.27×10^{-1}
-8	-1.14×10^{-1}	1.46	-4.15×10^{-2}	2.72×10^{-2}	1.30	-1.55	-4.17×10^{-1}

TABLE 3. Incremental contributions (see (3.14)) to the bulk electromigration of NaCl in a Brinkman medium with charged spherical inclusions: $a = 100 \text{ nm}$; $\ell \approx 0.951 \text{ nm}$; $T = 25^\circ\text{C}$; $D_1 \approx 1.33 \times 10^{-9} \text{ m}^2 \text{ s}^{-1}$ (Na^+); $D_2 \approx 2.03 \times 10^{-9} \text{ m}^2 \text{ s}^{-1}$ (Cl^-).

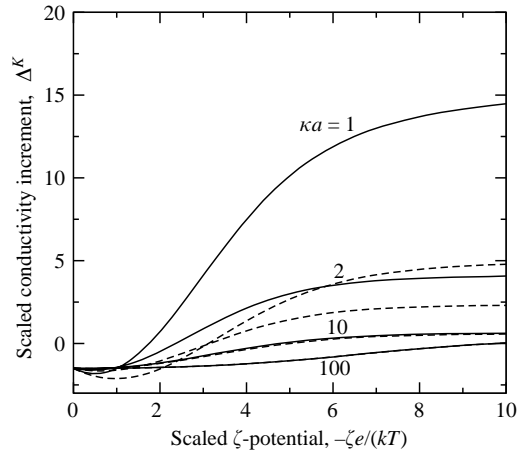


FIGURE 6. The (scaled) conductivity increment Δ^K (see (3.19)) as a function of the (scaled) ζ -potential $\zeta e/(kT)$ for various (scaled) reciprocal double-layer thicknesses $\kappa a = 1, 2, 10$ and 100 (aqueous NaCl at $T = 25^\circ\text{C}$ with $a = 100$ nm) for particles undergoing electrophoresis (solid lines) and stationary particles (dashed lines), both in electrolyte without polymer.

value $D^E = -(1/2)a^3$, so $\Delta^K \rightarrow -3/2$ as $|\zeta| \rightarrow 0$. In general, however, the conductivity increment also reflects the charge of the inclusions and the ionic strength.

Similarly to dispersions, the average convective term (involving C^E in (3.2)) does not influence the conductivity increment (because of electrical neutrality), and the diffusive term (involving C_j^E) vanishes only when the species have equal mobilities. In general, the (microscale) electromigrative and diffusive terms (involving D^E and C_j^E) contribute to the average current density. However, because these are influenced by fluid motion, the conductivity of a composite is not the same as when particles are fixed in an electrolyte without polymer. As expected, because only the electrolyte ions contribute to charge transfer, the conductivity of a composite is lower than when particles undergo electrophoresis.

Representative conductivity increments for mobile (solid lines) and stationary (dashed lines) particles in an NaCl electrolyte without polymer are compared in figure 6.† At low ionic strength (small κa), immobilizing the particles decreases the conductivity increment, because particle migration (electrophoresis) contributes significantly to charge transfer. At high ionic strength ($\kappa a > 10$), however, the conductivity increments for mobile and fixed particles are (practically) the same. This is because the density of charge added by the particles (macroions) is vanishingly small compared to the density of bulk electrolyte ions, so the conductivity reflects only the contribution of (dielectric and double-layer) polarization to the average electric field.

In contrast to KCl and HClO₄ electrolytes (see O'Brien 1981), the conductivity increment with NaCl decreases with increasing ζ -potential when ζ and κa are small. This may be attributed to the counter-ion (Na⁺) having a significantly lower mobility than the co-ion (Cl⁻). For KCl, the mobilities of K⁺ and Cl⁻ are very similar, yielding a monotonically increasing conductivity increment. For HClO₄, however, the counter-ion (H⁺) has a significantly higher mobility than the co-ion (ClO₄⁻), yielding

† The computations for particles in a pure electrolyte were performed with software (called MPEK, available from the author) based on the work of Hill *et al.* (2003). These accurately reproduced earlier calculations by O'Brien (1981) for KCl and HClO₄ electrolytes.

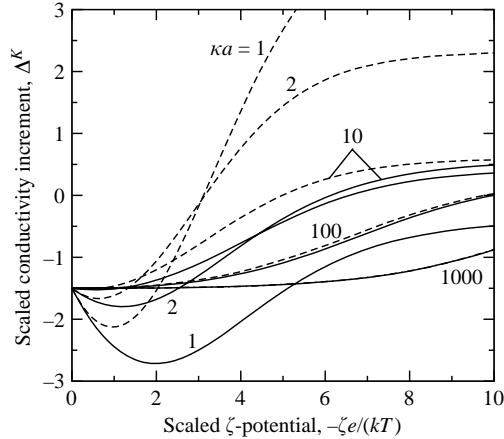


FIGURE 7. The (scaled) conductivity increment Δ^K (see (3.19)) as a function of the (scaled) ζ -potential $\zeta e/(kT)$ for various (scaled) reciprocal double-layer thicknesses $\kappa a = 1, 2, 10, 100$ and 1000 : aqueous NaCl at $T = 25^\circ\text{C}$; $a = 100$ nm; $\ell \approx 3.11$ (solid lines); stationary particles in electrolyte without polymer (dashed lines).

a conductivity increment that increases more rapidly (linearly) with $|\zeta|$ (see O'Brien 1981).

The conductivity increment for particles with radius $a = 100$ nm embedded in a polymer gel with Brinkman screening length $\ell \approx 3.11$ nm (solid lines) is shown in figure 7. Similar calculations (not shown) reveal that an order-of-magnitude increase in the permeability ℓ^2 produces almost the same values at all ζ -potentials and ionic strengths (values of κa). This confirms that the average current density is dominated by electromigration and diffusion. The conductivity increments (solid lines) are compared to values for stationary particles in an electrolyte without polymer (dashed lines). These results are almost the same at high ionic strength when the diffuse double layer is thin compared to the Brinkman screening length, i.e. when $\kappa \ell \gg 1$. Under these conditions, the electrical force (inside the diffuse double layer) is balanced by viscous stress and, hence, the convective flows are similar. When $\kappa \ell = \kappa a(\ell/a) = 1$, for example, $\kappa a \approx 100/3.11 \approx 32$ and, as expected, the limiting behaviour ($\kappa \ell \gg 1$) at high ionic strength occurs when κa exceeds this value.

4. Summary

A rigorous theoretical methodology has been presented to calculate steady electrokinetic transport of electrolytes in a continuous polymer gel embedded with charged spherical inclusions. Composites with this microstructure are candidates for enhanced gel-electrophoresis, chemical sensing, membrane separation, and, perhaps, electro-osmotic pumping technologies. This work was also motivated by a desire to interpret experiments that probe the surface charge of immobilized colloids and the micro-rheology of delicate polymer gels.

From a numerically exact treatment of electromigration, diffusion, and convective transport past a single inclusion in an unbounded polymer gel, averaged equations describing bulk transport properties were derived. The theory was applied to calculate the response to a steady electric field with a uniform bulk electrolyte concentration. Note that the response to a bulk electrolyte concentration gradient is treated in a companion paper (Hill 2006). In this work, electromigration and diffusion were found

to be independent of convection and, hence, of the polymer-gel (Darcy) permeability. However, the strength of electro-osmotic flow reflects the gel permeability and, to a lesser (but still significant) extent, polarization and relaxation by electromigration and diffusion.

When particles are immobilized in a (neutral) polymer gel, the electrical conductivity is independent of the polymer, whereas the pore mobility – similarly to the electrophoretic mobility of dispersions – reflects the size and charge of the inclusions *and* the Darcy permeability. Furthermore, when the Debye length is smaller (greater) than the Brinkman screening length ℓ (square root of the Darcy permeability), the pore mobility increases linearly (quadratically) with ℓ .

The variation of pore mobility with ζ -potential and ionic strength is more complicated because of the significant influence of polarization and relaxation. Nevertheless, the mobility is (approximately) inversely proportional to the inclusion radius, indicating, as expected, that the average flow is proportional to the average counter-charge density in the composite.

The Darcy drag of the intervening polymer gel leads to slow flows that will often be independent of the differential pressure required to pump fluid through a (modest) microfluidic network. Optimal pumping efficiency is favoured by thin membranes with large cross-section, high inclusion volume fractions, and low electrolyte conductivities.

The present model assumes that the polymer gel does not influence ion mobilities (diffusion coefficients), and that the volume fraction of the inclusions is small. By analogy with Maxwell's well-known theory for conduction in dilute random arrays of spheres, the theory advanced in this work may be accurate at moderate volume fractions. Note also that the calculations require the bulk electrostatic potential and electrolyte ion concentrations to vary slowly in space (and time). Future development of the model will accommodate harmonic temporal fluctuations in the applied electric field, permitting the interpretation of dielectric relaxation spectroscopy experiments.

Supported by the Natural Sciences and Engineering Research Council of Canada (NSERC), through grant number 204542, and the Canada Research Chairs program (Tier II). The author thanks I. Ispolatov (University of Santiago) for fruitful discussions related to this work, and an anonymous referee for helpful suggestions.

Appendix. Derivation of the averaged momentum equation

This Appendix supplements §2.4 where the single-particle microscale problem is adopted to quantify the influence of the inclusions on bulk momentum transport. Note that the closures in this work neglect hydrodynamic interactions between inclusions, which are screened by the intervening Brinkman medium. The reader is referred to Hinch (1977) for details necessary to account for hydrodynamic interactions. Note also that the fields obtained from the single-particle problem in this work approximate the conditionally averaged fields in Hinch's ensemble averaging methodology. Because the microstructure is homogeneous, the volume averages below are equivalent to ensemble averages. Integrals over the surface or volume of a (spherical) inclusion centred at $r=0$ are identified by a range of integration that involves the radial coordinate r ; otherwise integrals refer to 'representative control volumes'. Unless stated otherwise, the notation and symbols below are the same as in the main text.

Outside the inclusions, the (inertialess) microscale momentum conservation equation is

$$\mathbf{0} = \nabla \cdot \mathbf{T} - (\eta/\ell^2)\mathbf{u} - \rho\nabla\psi + \rho_f\mathbf{g}, \quad (\text{A } 1)$$

where $\mathbf{T} = -p\mathbf{I} + 2\eta\mathbf{e}$ is the Newtonian stress tensor, ρ_f is the fluid density, $\rho_f\mathbf{g}$ is a uniform body force (e.g. gravity), and p is the change density.

Similarly, let the microscale momentum conservation equation inside the (rigid) inclusions be

$$\mathbf{0} = \nabla \cdot \mathbf{T}^p + \rho_p\mathbf{g} + \mathbf{f}^s, \quad (\text{A } 2)$$

where \mathbf{T}^p is the stress tensor, and ρ_p is the particle density. Note that \mathbf{f}^s is a *generalized function* to represent the electrical and mechanical-contact forces acting on the surfaces of the inclusions: $\mathbf{f}^s = \mathbf{0}$ when $r \neq a$, and

$$V^{-1} \int_V \mathbf{f}^s dV = n \langle \mathbf{f}^s \rangle \quad (\text{A } 3)$$

when $nV \gg 1$ and $V^{1/3}$ is small compared to the characteristic macroscopic length scale.

Averaging the momentum conservation equation yields Brinkman's equation for the continuous phase (fluid-saturated polymer gel), with additional terms arising from the inclusions:

$$\begin{aligned} \mathbf{0} = & \nabla \cdot \langle \mathbf{T} \rangle - (\eta/\ell^2) \langle \mathbf{u} \rangle - \langle \rho \nabla \psi \rangle + \rho_f \mathbf{g} \\ & + \nabla \cdot \left\{ n \left\langle \int_{r < a} (\mathbf{T}^p + p\mathbf{I}) dV \right\rangle \right\} + n \langle \mathbf{f}^s \rangle + \phi(\rho_p - \rho_f) \mathbf{g}. \end{aligned} \quad (\text{A } 4)$$

Note that $\langle \rho \nabla \psi \rangle$ includes only the counter-charge; the influence of the fixed surface charge is captured by $\langle \mathbf{f}^s \rangle$, which is the sum of the average electrical $\langle \mathbf{f}^e \rangle$ and mechanical-contact $\langle \mathbf{f}^m \rangle$ forces acting on the surfaces of the inclusions (or more generally inside). Accordingly, the (averaged) equation of static equilibrium for the (immobilized) inclusions is

$$n \langle \mathbf{f}^d \rangle + n \langle \mathbf{f}^s \rangle + \phi \rho_p \mathbf{g} = \mathbf{0}, \quad (\text{A } 5)$$

where

$$\langle \mathbf{f}^d \rangle = \left\langle \int_{r=a} \mathbf{T} \cdot \mathbf{e}_r dA \right\rangle \quad (\text{A } 6)$$

is the average (drag) force exerted by the fluid on the inclusions.

A useful identity for transforming volume to surface integrals is obtained by differentiating the product (summation on repeated indices)

$$\partial(\alpha_{klm\dots} x_i) / \partial x_j = x_i \partial \alpha_{klm\dots} / \partial x_j + \alpha_{klm\dots} \delta_{ij}, \quad (\text{A } 7)$$

where $\alpha_{klm\dots}$ are the components of an arbitrary-order tensor (e.g. stress). Integrating this over a volume $\int dV$ enclosed by a surface $\int dA$ and applying Gauss's integral theorem gives

$$\int \alpha_{klm\dots} dV = \int x_i \alpha_{klm\dots} \hat{n}_j dA - \int x_i \partial \alpha_{klm\dots} / \partial x_j dV. \quad (\text{A } 8)$$

Therefore, with $\mathbf{T}^p = \mathbf{T}$ at $r = a$, and $\nabla \cdot \mathbf{T}^p = -\rho_p \mathbf{g}$ and $\mathbf{e} = \mathbf{0}$ (rigid particles) when $r < a$, it follows that

$$\left\langle \int_{r < a} (\mathbf{T}^p + p\mathbf{I}) dV \right\rangle = \left\langle \int_{r=a} \mathbf{r} 2\eta \mathbf{e} \cdot \mathbf{e}_r dA \right\rangle. \quad (\text{A } 9)$$

In general, body forces and the isotropic stress contribute $\langle \int \mathbf{r} (\mathbf{f}^s + \rho_p \mathbf{g} - \nabla p) dV \rangle$ to the right-hand side of (A 9), but these integrals vanish if, on average, the

(internal) body-force distributions and (internal) pressure gradient are even functions of position. With a macroscale velocity gradient (not considered in this work), the extensional and rotational contributions to \mathbf{e} are even functions of position, so $\langle \int_{r=a} \mathbf{r} \mathbf{e} \cdot \mathbf{e}_r \, dA \rangle$ will be linear in $\langle \nabla \mathbf{u} \rangle$ and, therefore, will contribute to the bulk (deviatoric) stress by modifying the effective viscosity η' (e.g. the well-known Einstein viscosity for dilute, force-free suspensions).

Finally, collecting the results from (A 4)–(A 9) gives

$$\mathbf{0} = \nabla \cdot \langle \mathbf{T} \rangle - (\eta/\ell^2) \langle \mathbf{u} \rangle - \langle \rho \nabla \psi \rangle + (1 - \phi) \rho_f \mathbf{g} + \nabla \cdot \left\{ n 2\eta \left\langle \int_{r=a} \mathbf{r} \mathbf{e} \cdot \mathbf{e}_r \, dA \right\rangle \right\} - n \langle \mathbf{f}^d \rangle. \quad (\text{A } 10)$$

The correctness of (A 10) can be verified, in part, by considering a stationary fixed bed of inclusions in the absence of electrical forces. Accordingly, (A 10) simplifies to

$$\mathbf{0} = -\nabla \langle p \rangle + (1 - \phi) \rho_f \mathbf{g} - n \langle \mathbf{f}^d \rangle,$$

and the static equilibrium of the inclusions requires

$$\mathbf{0} = n \langle \mathbf{f}^d \rangle + n \langle \mathbf{f}^s \rangle + \phi \rho_p \mathbf{g}. \quad (\text{A } 11)$$

Therefore,

$$\mathbf{0} = -\nabla \langle p \rangle + n \langle \mathbf{f}^s \rangle + \rho_f \mathbf{g} + \phi (\rho_p - \rho_f) \mathbf{g}, \quad (\text{A } 12)$$

and, hence, in a stationary fluid where $\nabla \langle p \rangle = \rho_f \mathbf{g}$, the average force required to immobilize the inclusions is simply

$$\langle \mathbf{f}^s \rangle = (\phi/n) (\rho_f - \rho_p) \mathbf{g} = (4/3) \pi a^3 (\rho_f - \rho_p) \mathbf{g}. \quad (\text{A } 13)$$

REFERENCES

- BOOTH, F. 1950 The cataphoresis of spherical, solid non-conducting particles in a symmetrical electrolyte. *Proc. R. Soc. Lond.* **203**, 533–551.
- BRINKMAN, H. C. 1947 A calculation of the viscous force exerted by a flowing fluid on a dense swarm of particles. *Appl. Sci. Res. A* **1**, 27–34.
- DE LACEY, E. H. B. & WHITE, L. R. 1981 Dielectric response and conductivity of dilute suspensions of colloidal particles. *J. Chem. Soc., Faraday Trans. II* **77**, 2007–2039.
- DUKHIN, S., ZIMMERMAN, R. & WERNER, C. 2004 Intrinsic charge and Donnan potentials of grafted polyelectrolyte layers determined by surface conductivity data. *J. Colloid Interface Sci.* **274**, 309–318.
- HILL, R. J. 2004 Hydrodynamics and electrokinetics of spherical liposomes with coatings of terminally anchored poly(ethylene glycol): Numerically exact electrokinetics with self-consistent mean-field polymer. *Phys. Rev. E* **70**, 051406.
- HILL, R. J. 2006 Transport in polymer-gel composites: response to a bulk concentration gradient. *J. Chem. Phys.* **124**, 014901.
- HILL, R. J. & SAVILLE, D. A. 2005 ‘Exact’ solutions of the full electrokinetic model for soft spherical colloids: Electrophoretic mobility. *Colloids Surfaces A: Physicochem.* **267**, 31–49.
- HILL, R. J., SAVILLE, D. A. & RUSSEL, W. B. 2003 Electrophoresis of spherical polymer-coated colloidal particles. *J. Colloid Interface Sci.* **258**, 56–74.
- HINCH, E. J. 1977 An averaged-equation approach to particle interactions in a fluid suspension. *J. Fluid Mech.* **83**, 695–720.
- HUNTER, R. J. 2001 *Foundations of Colloid and Interface Science*, 2nd edn. Oxford University Press.
- KOCH, D. L. & SANGANI, A. S. 1999 Particle pressure and marginal stability limits for a homogeneous monodisperse gas fluidized bed: kinetic theory and numerical simulations. *J. Fluid Mech.* **400**, 229–263.

- O'BRIEN, R. W. 1981 The electrical conductivity of a dilute suspension of charged particles. *J. Colloid Interface Sci.* **81**, 234–248.
- O'BRIEN, R. W. 1988 Electro-acoustic effects in a dilute suspension of spherical particles. *J. Fluid Mech.* **190**, 71–86.
- O'BRIEN, R. W. 1990 The electroacoustic equations for a colloidal suspension. *J. Fluid Mech.* **212**, 81–93.
- O'BRIEN, R. W. & WHITE, L. R. 1978 Electrophoretic mobility of a spherical colloidal particle. *J. Chem. Soc., Faraday Trans. II* **74**, 1607–1626.
- OVERBEEK, J. T. G. 1943 Theorie der elektroforese. *Kolloid-Beih.* **54**, 287–364.
- RUSSEL, W. B., SAVILLE, D. A. & SCHOWALTER, W. R. 1989 *Colloidal Dispersions*. Cambridge University Press (paperback edition 1991).
- SAVILLE, D. A. 1979 Electrical conductivity of suspensions of charged particles in ionic solutions. *J. Colloid Interface Sci.* **71**, 477–490.
- SAVILLE, D. A. 1982 The sedimentation potential in a dilute suspension. *Adv. Colloid Interface Sci.* **16**, 267–279.
- SAVILLE, D. A. 2000 Electrokinetic properties of fuzzy colloidal particles. *J. Colloid Interface Sci.* **222**, 137–145.
- YAO, S., HERTZOG, D. E., MIKKELSEN, J. C. J. & SANTIAGO, J. G. 2003 Porous glass electro-osmotic pumps: design and experiments. *J. Colloid Interface Sci.* **268**, 143–153.
- YAO, S. & SANTIAGO, J. G. 2003 Porous glass electro-osmotic pumps: theory. *J. Colloid Interface Sci.* **268**, 133–142.